Received: 5 January 2021 | Revised: 11 April 2021 | Accepted: 14 April 2021

DOI: 10.1111/mec.15924

ORIGINAL ARTICLE

MOLECULAR ECOLOGY WILEY

Volcanism and palaeoclimate change drive diversification of the world's largest whip spider (Amblypygi)

Frederic D. Schramm[1] | **Alejandro Valdez-Mondragón**[2] | **Lorenzo Prendini**[1]

[1]Arachnology Lab, Division of Invertebrate Zoology, American Museum of Natural History, New York, NY, USA

[2]Laboratory of Arachnology (LATLAX), Laboratorio Regional de Biodiversidad y Cultivo de Tejidos Vegetales (LBCTV), Instituto de Biología, Universidad Nacional Autónoma de México (UNAM), sede Tlaxcala, Tlaxcala, Mexico

Correspondence
Frederic D. Schramm, Arachnology Lab, Division of Invertebrate Zoology, American Museum of Natural History, New York, NY, USA.
Email: frederic.d.schramm@gmail.com

Funding information
Deutscher Akademischer Austauschdienst; Laboratorio Regional de Biodiversidad y Cultivo de Tejidos Vegetales del Instituto Biología, Universidad Nacional Autónoma de México, sede Tlaxcala; Division of Environmental Biology, Grant/Award Number: 2003382; Theodore Roosevelt Memorial Fund of the American Museum of Natural History; Consejo Nacional de Ciencia y Tecnología

Abstract

The tropics contain many of the most biodiverse regions on Earth but the processes responsible for generating this diversity remain poorly understood. This study investigated the drivers of diversification in arthropods with stenotopic ecological requirements and limited dispersal capability using as a model the monotypic whip spider (Amblypygi) genus *Acanthophrynus*, widespread in the tropical deciduous forests of Mexico. We hypothesized that for these organisms, the tropical deciduous forests serve as a conduit for dispersal, with their disappearance imposing barriers. Given that these forests are located in a region of complex geological history and that they fluctuated in extent during the Pliocene–Pleistocene glacial/interglacial cycles we combine molecular divergence dating, palaeoclimatic niche modelling and ancestral area reconstruction to test if and when habitat fragmentation promoted diversification in *Acanthophrynus*. Concomitant with the expected role of landscape change, we demonstrate that orogeny of the Trans-Mexican Volcanic Belt, in the Late Miocene or Early Pliocene (6.95–5.21 million years ago), drove the earliest divergence of *Acanthophrynus* by vicariance. Similarly, as expected, the later onset of glaciations strongly impacted diversification. Whereas a more stable climate in the southern part of the distribution enabled further diversification, a marked loss of suitable habitat during the glaciations only allowed dispersal and diversification in the north to occur later, resulting in a lower overall diversity in this region. Barriers and diversification patterns identified in *Acanthophrynus* are reflected in the phylogeography of codistributed vertebrates and arthropods, emphasizing the profound impact of Trans-Mexican Volcanic Belt orogeny and glacial/interglacial cycles as drivers of diversification in the Mexican Neotropics.

KEYWORDS
biogeography, cryptic diversity, divergence dating, environmental niche modelling, glacial/interglacial cycles, Trans-Mexican Volcanic Belt

1 | INTRODUCTION

The tropics contain many of the most biodiverse regions on Earth but the processes responsible for generating this diversity remain poorly understood (Fine, 2015; Smith et al., 2014). One hypothesis for the drivers of tropical diversification contends that terrestrial tropical biomes covered larger areas, for a longer period of time, providing more spatiotemporal opportunity for diversification (Fine & Ree, 2006; Wiens & Donoghue, 2004). Adaptation to new environments and ecological roles, usually associated with morphological or physiological innovation, is an important driver of diversification, increasing the rate of speciation and often culminating in adaptive

radiation (Gillespie et al., 2020; Simões et al., 2016). Major changes to the landscape, such as orogeny and the formation or alteration of river drainages, frequently associated with tectonic forces, promote allopatric speciation through vicariance (Hoorn et al., 2010; Simões et al., 2016; Smith et al., 2014). The role of orogeny may be especially pronounced in the tropics due to the often narrower niches and more stenotopic ecological requirements of tropical taxa (Ghalambor, 2006; Janzen, 1967; Sheldon et al., 2018; Stevens, 1989; Vázquez & Stevens, 2004), leading to a greater propensity for vicariance with increased elevation. Superimposed on landscape changes, habitat fragmentation associated with climate fluctuations may further promote allopatric speciation, especially in stenotopic tropical taxa (Garzón-Orduña et al., 2014; Hoorn et al., 2010).

At the convergence of the Nearctic and Neotropical realms, separated by major mountain ranges with biotic assemblies of transitional character (Halffter & Morrone, 2017; Morrone, 2020), Mexico represents an understudied laboratory of tropical diversification. The complex history of the Mexican landscape was dominated by the orogeny of the Sierras and cyclical fluctuations in climate that produced its diverse biomes, which vary from desert to rainforest, often over short distances (Morrone, 2020). The Mexican Neotropics is a biodiversity hotspot subdivided into four biogeographical provinces (Morrone et al., 2017). The Yucatán Peninsula and Veracruz provinces in the east are dominated by evergreen tropical forests. The Balsas Depression in central Mexico and the Pacific Lowlands Province in western Mexico contain some of the world's largest tropical deciduous forests (Sosa et al., 2018). Compared to other seasonally dry tropical forests, these forests are especially speciose and considered a conservation priority (Gentry, 1995; Olson et al., 2001). Four ecoregions are recognized in the Mexican Pacific Lowlands: the Sinaloan, Jalisco, Southern Pacific and Central American Dry Forest ecoregions (Olson et al., 2001) (Figure 1a).

The orogeny of the Trans-Mexican Volcanic Belt, which began in the Miocene, and the glacial/interglacial cycles of the Pliocene–Pleistocene appear to have been major drivers of diversification in Mexico, but affected different taxa in different ways (Bryson et al., 2011; Mastretta-Yanes et al., 2015). Research on reptiles, amphibians and freshwater fish has shown varying levels of agreement with currently defined biogeographical boundaries in the Mexican Neotropics (Mateos et al., 2002; Suárez-Atilano et al., 2014; Zarza et al., 2008). Although arthropods such as beetles played an important role in hypotheses concerning the origin and diversification of the Mexican biota (Morrone & Márquez, 2001), few studies have investigated the phylogeography or molecular phylogeny of arthropod taxa inhabiting the tropical deciduous forests of the Balsas Depression and the Pacific Lowlands provinces (Nolasco-Soto et al., 2017; Pringle et al., 2012; Rengifo-Correa et al., 2021).

Due to limited vagility, more stenotopic ecological requirements and narrower ranges (Clouse et al., 2016; Ferrier et al., 1999), terrestrial arthropods may be more sensitive to habitat fragmentation, diversifying earlier and/or more extensively than vertebrates in response to vicariance events associated with broad landscape modifications or climatic fluctuations. As such, arthropods are particularly well suited for assessing the role of the landscape and climate fluctuations as drivers of diversification compared to vertebrates, on which the majority of such studies have been conducted (Ferrier et al., 1999; Loria & Prendini, 2020). Additionally, genetic studies routinely reveal that arthropod diversity has been underestimated (Stork, 2018), suggesting arthropods can provide more granular resolution of diversity and diversification.

Whip spiders (Amblypygi Thorell, 1883), an order of tropical arachnids related to spiders (Weygoldt, 2000), which reach their greatest diversity in the Mexican Neotropics (Armas, 2006; Harvey, 2003), offer a model system to address the drivers of tropical diversification. Unlike spiders, most of which are capable of dispersal on air currents (Weyman, 1993), whip spiders are limited to walking and possibly rafting (Chapin et al., 2018). Their vagility is further constrained by an ecological requirement for humidity, which restricts them to forests, caves or the vicinity of permanent water sources in arid areas (Weygoldt, 2000). Although phylogeographical studies of whip spiders remain scarce, the few published to date confirm that their diversity is underestimated and informative for understanding diversification in the tropics (Chapin et al., 2018; Esposito et al., 2015; Prendini et al., 2005; Reveillion et al., 2020).

The present study uses *Acanthophrynus coronatus* (Butler, 1873), the world's largest whip spider (Quintero, 1980), as a model to test the role of vicariance and dispersal in tropical diversification by investigating its phenotypic diversity, phylogeography and environmental niche space. This species, the sole member of the genus *Acanthophrynus* Kraepelin, 1899, is distributed throughout the tropical deciduous forests of Mexico. Colour variation among allopatric populations of *Acanthophrynus* suggests some degree of phenotypic diversification across its distribution (Quintero, 1980), possibly reflecting the divergence of lineages in the phylogeny. As *Acanthophrynus* is restricted to tropical deciduous forests and whip spiders generally display stenotopic ecological requirements (Weygoldt, 2000), implying narrow environmental niches, we hypothesized that environmental adaptation to new or changing habitats is not a primary driver of diversification. As such, we do not expect phylogenetic divergence to correlate strongly with distance in environmental space in *Acanthophrynus*. Instead, we hypothesize that tropical deciduous forests served as a conduit for dispersal, their disappearance, by landscape or palaeoclimatic change, imposing barriers that promoted diversification by vicariance.

The Trans-Mexican Volcanic Belt, the orogeny of which began in the Miocene, drove the divergence of codistributed vertebrates in the late Miocene or Pliocene (Suárez-Atilano et al., 2014; Zarza et al., 2008). We hypothesize that the emergence of this mountain chain, which bisects the distribution of *Acanthophrynus*, also drove diversification by vicariance in these whip spiders. Using ancestral area reconstruction and molecular divergence dating, we expect divergence of *Acanthophrynus* in the Late Miocene or Pliocene to coincide with a predicted vicariance event in an area of Trans-Mexican Volcanic Belt orogeny. Further, as the distribution of *Acanthophrynus* covers a large latitudinal gradient, its range extending 1300 km from

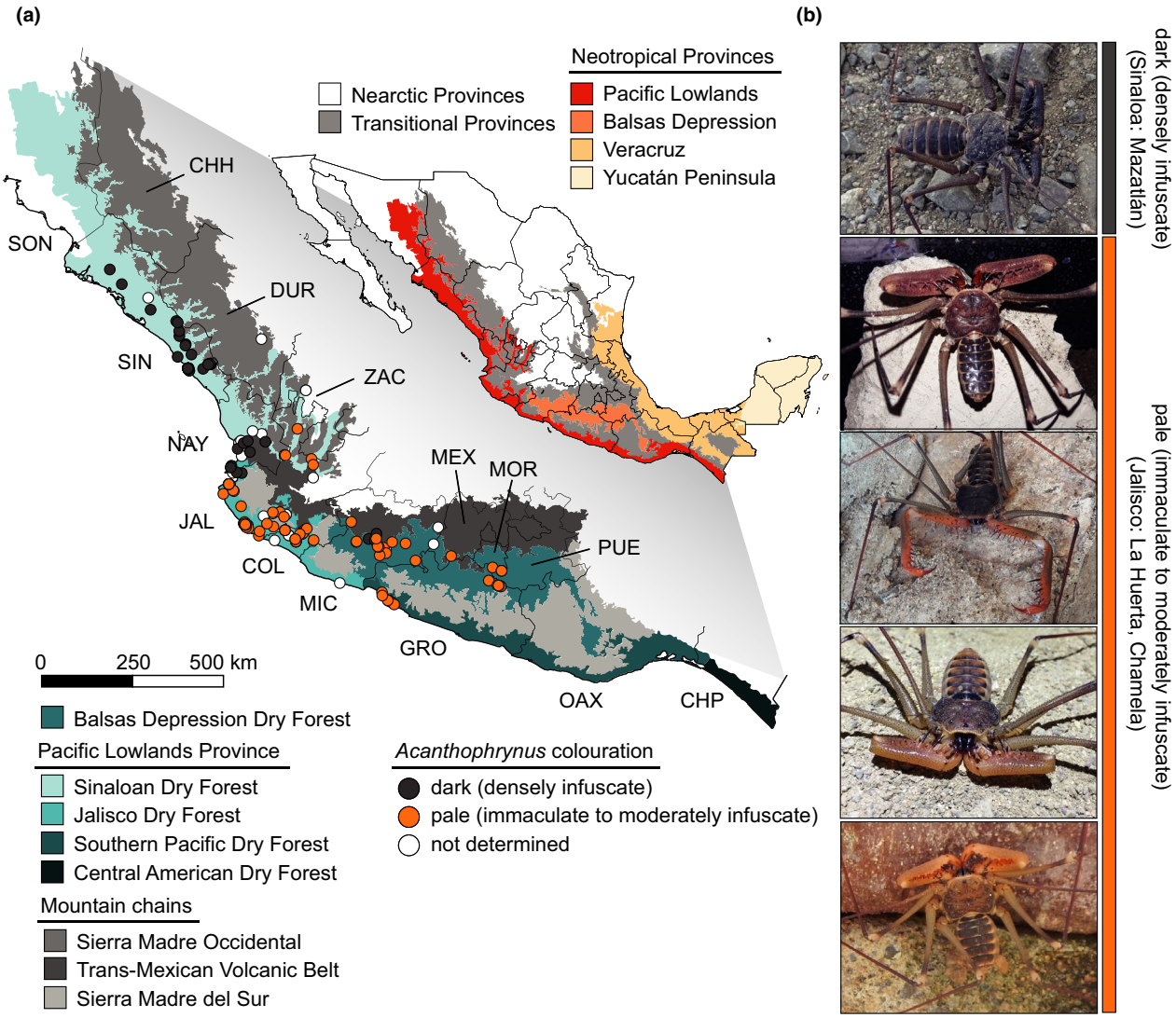

FIGURE 1 Distribution of colour variation among populations of *Acanthophrynus* whip spiders (Amblypygi) in the Mexican Neotropics. (a) Nearctic, Transitional and Neotropical biogeographical provinces of Mexico (smaller map) and western Mexico indicating ecoregions and records of dark and pale populations. Mexican states abbreviated as follows: CCH, Chihuahua; CHP, Chiapas; COL, Colima; DUR, Durango; GRO, Guerrero; JAL, Jalisco; MEX, México; MIC, Michoacán; MOR, Morelos; NAY, Nayarit; OAX, Oaxaca; PUE, Puebla; SIN, Sinaloa; SON, Sonora; ZAC, Zacatecas. (b) Live habitus with varying degrees of infuscation. Densely infuscate specimen from Mazatlán, central Sinaloa (courtesy of D. Barrales-Alcalá); specimens ranging from moderately infuscate to immaculate (top to bottom) from Chamela, central coastal Jalisco (top two from the second author, second from bottom courtesy of D. Vivar, bottom courtesy of M. Mejía-Duque)

Sinaloa, in the north, along the Pacific coast, and inland to the eastern Balsas Depression, in Guerrero (Armas, 2006), we predict currently inhabited regions to have differed markedly in suitable habitat during the Pliocene–Pleistocene glaciations. In accordance with the notion that less pronounced climate fluctuations in the tropics provided more opportunity for diversification in these biomes (Fine & Ree, 2006; Wiens & Donoghue, 2004), we hypothesize that the geographical distribution of diversity in *Acanthophrynus* will reflect the local continuity of suitable habitat through time in environmental niche models. We expect less diversification and later dispersal into northern areas which probably experienced drastic reductions in suitable habitat during glacial periods. On the other hand, we expect greater genetic distances among populations from areas in which the habitat remained more stable, and diversification might have been driven by localized habitat fragmentation.

Finally, we hypothesize that landscape and climatic change-induced diversification patterns in *Acanthophrynus* will be reflected in the phylogeography of codistributed vertebrates and arthropods. Although some variation between divergence times and genetic divergence are to be expected based on the different properties of these organisms, we expect to identify similar genetic boundaries reflecting common barriers. Further, given its unusually wide distribution for a single arthropod species, vicariance events associated with habitat fragmentation in *Acanthophrynus* may have caused levels of genetic divergence similar to those observed between morphologically distinct species of codistributed arthropods.

2 | MATERIALS AND METHODS

2.1 | Material, locality records and distribution mapping

Preserved specimens were obtained from eight museum collections (Appendix S1). Tissue samples are deposited in the Ambrose Monell Cryocollection (AMCC) at the American Museum of Natural History (AMNH). Specimen labels or database entries without geographical coordinates were retroactively georeferenced using Google Earth (Table S1). In addition to museum material, 221 geographical occurrence records of *Acanthophrynus* were retrieved from the citizen science platform iNaturalist (https://www.inaturalist.org). After inspection of photographs associated with the records, 38 records were rejected as misidentified, unidentifiable or with a reported positional accuracy greater than 20 km. The final set of 242 occurrence records used for the analyses is summarized in Table S1.

Geographical maps were generated in QGIS version 3.10 (https://www.qgis.org). SRTM raster elevation data (30 s) (Farr et al., 2007) were obtained from WorldClim version 2.1 (https://www.worldclim.org/data/worldclim21.html; Fick & Hijmans, 2017). Shapefiles delineating country administrative boundaries were downloaded from the Humanitarian Data Exchange Platform version 1.39.4 (https://data.humdata.org/), shapefiles of terrestrial ecoregions (Olson et al., 2001) from the WWF (https://www.worldwildlife.org/publications/terrestrial-ecoregions-of-the-world), and shapefiles of Mexican biogeographical provinces according to Morrone et al. (2017) from the Conservation Biogeography Group at the Universidad Nacional Autonóma de México (http://mexicanmap.atlasbiogeografico.com).

2.2 | *Acanthophrynus* colouration and environmental space

The colouration of *Acanthophrynus* was assessed from iNaturalist photographs by separately scoring the density of infuscation of the pedipalps, carapace and tergites. Mapping colour variations revealed that orange (immaculate) or light brown (sparsely infuscate) pedipalps co-occurred with a light brown (sparsely infuscate) or dark brown (moderately infuscate) carapace in the same or neighbouring populations throughout the Jalisco Dry Forest and Balsas Depression Dry Forest whereas blackish (densely infuscate) pedipalps and carapace occurred in the coastal regions of Nayarit (Jalisco Dry Forest) and the Sinaloan Dry Forest (Figure S1). Therefore, only two colour variations of *Acanthophrynus* were considered further: (i) populations in which carapace, pedipalps and tergites are blackish (densely infuscate), referred to as "dark"; and (ii) populations in which pedipalps vary from orange to light brown (immaculate to sparsely infuscate) whereas carapace and tergites vary from light to dark brown (sparsely to moderately infuscate), collectively referred to as "pale." This approach enabled colouration to be assessed in ethanol-preserved material, excluding old or degraded material (Table S1).

Occurrence records were associated with one of three ecoregions (Olson et al., 2001): Sinaloan Dry Forest (SDF); Jalisco Dry Forest (JDF) and Southern Pacific Dry Forest (SPDF); and Balsas Depression Dry Forest (BDDF) (Table S1). Contemporary climate data (1960–1990) from Worldclim version 1.4 (Hijmans et al., 2005), comprising 19 rasters of hydrothermal bioclimatic covariates at a resolution of 2.5 arc-minutes, were used to characterize the environment of *Acanthophrynus*. Occurrence records were trimmed of exact georeferenced duplicates and corresponding values of environmental covariates extracted from rasters using the R package RASTER (Hijmans & Van Etten, 2020). Present-day per-occurrence values (including phenotypically assessed and nonassessed records) of the 19 covariates were used to perform a principal components analysis (PCA) using the R package STATS (R Core Team, 2012). The individual contributions of covariates to the principal components are summarized in Table S2. Environmental values were extracted from 19 raster layers of different palaeoclimate scenarios, derived from general circulation models (https://www.worldclim.org/data/v1.4/paleo1.4.html): mid-Holocene (~6 thousand years ago [ka]): CCSM4 (Gent et al., 2011), MIROC-ESM (K-1 Model Developers, 2004), and MPI-ESM-P (Stevens et al., 2013) at 2.5 arc-minutes; the Last Glacial Maximum (~22 ka): CCSM4 (Gent et al., 2011), MIROC-ESM (K-1 Model Developers, 2004), and MPI-ESM-P (Stevens et al., 2013) at 2.5 arc-minutes; and the last interglacial (~140–120 ka): NCAR-CCSM (Otto-Bliesner et al., 2006) at 30 arc-seconds.

2.3 | Environmental niche modelling

Environmental niche models were generated with MAXENT version 3.4.1 (Phillips et al., 2006, 2017; Phillips & Dudík, 2008) using an R-based modular workflow on the Wallace platform (Kass et al., 2018) and further customized. After removing duplicates, occurrence records were spatially thinned using the R package SPTHIN (Aiello-Lammens et al., 2015), applying a thinning distance of 10 km to reduce spatial sampling bias. The set of contemporary climate data (1960–1990), comprising 19 rasters of hydrothermal bioclimatic covariates at a resolution of 2.5 min, from Worldclim version 1.4 (Hijmans et al., 2005), was used. Models were generated using two approaches: including all 19 bioclim predictors without addressing predictor collinearity; and using environmental layers of uncorrelated principal components. NICHEA version 3.0.12 (Qiao et al., 2016) was used to obtain a derived set of environmental rasters based on a PCA of the contemporary 19 bioclimatic covariate raster layers, cropped to the area of Mexico. The PCA was transferred to the rasters of different palaeoclimate scenarios. The first five principal components accounted for 95% of the total variance observed in rasters of the original variables (PC1, 46.77%; PC2, 23.21%; PC3, 13.34%; PC4, 7.85%; PC5, 3.5%) and the corresponding rasters were selected for modelling.

The background extent used to mask different sets of predictor variable layers based on the occurrence data, from which 10,000 pseudo-absences were randomly sampled, was defined as 1.3°

occurrence point buffers and calculated with the R package DISMO (Hijmans et al., 2020). The complexity and predictive power of the models were optimized using the R package ENMEVAL (Muscarella et al., 2014). The geographical "block" partitioning scheme was used to generate models for six regularization multiplier values (from 1 to 3, with increments of 0.5) for which all feature classes and combinations in the Wallace tool (L, LQ, H, LQH, LQHP) were tested. Models with a model omission rate calculated with the tenth percentile and minimum training presence thresholds ≤1.5 times the lowest value were subsetted and the model with lowest corrected Akaike Information Criterion, selected. Models were projected (allowing clamping). The degree to which extrapolation affected predictions was assessed by multivariate environmental similarity surfaces (Elith et al., 2010) using DISMO.

Niche overlap between two projections was assessed by calculating the *D* statistic using DISMO (Schoener, 1968) and *I*, a measure derived from the Hellinger distance (Van der Vaart, 1998), as described in Warren et al. (2008). Identity and background tests (Warren et al., 2008, 2010), each based on 50 pseudoreplicated data sets each, were performed using a custom script.

2.4 | DNA sequencing and alignment

The ingroup comprised 26 specimens of *Acanthophrynus* from 16 localities (a proxy for populations), covering most of the distribution (Table 1). One specimen each of *Phrynus marginemaculatus* C.L. Koch, 1840, *Paraphrynus laevifrons* (Pocock, 1894) and *Heterophrynus longicornis* (Butler, 1873), representing the other three genera of the whip spider family Phrynidae Blanchard, 1852, were included as outgroups (Table 1). The tree was rooted on *H. longicornis*, representing Heterophryninae Pocock, 1902, the sister group of the nominotypical subfamily Phryninae Blanchard, 1852, to which the other three genera belong (Weygoldt, 2000).

DNA extraction, PCR (polymerase chain reaction) and Sanger dideoxy sequencing were performed at the AMNH Sackler Institute of Comparative Genomics (SICG), using standard protocols (Prendini et al., 2005). Three nuclear gene markers, 18S rDNA (18S), 28S rDNA (28S), and a region spanning the Internal Transcribed Spacer 1, 5.8S rDNA and Internal Transcribed Spacer 2 (ITS1/2), and three mitochondrial gene markers, 12S rDNA (12S), 16S rDNA (16S) and cytochrome *c* oxidase subunit I (COI), were selected for efficacy in reconstructing the phylogeny of whip spiders (Chapin et al., 2018; Esposito et al., 2015; Harrison et al., 2017; Prendini et al., 2005). Loci were amplified using universal primers and/or, in the case of COI, 28S and ITS1/2, with primers specifically designed for *Acanthophrynus* (Tables S3 and S4). Sequence trace files were assembled into contigs and trimmed in GENESTUDIO PRO version 2.2.0.0 (http://genestudio.com/node/56).

DNA sequences were generated for all *Acanthophrynus* samples and the three outgroups in the case of the 12S, 16S and COI markers. ITS1/2 and 28S sequences could not be amplified for two and three *Acanthophrynus* samples, respectively. 18S sequences were generated for the three outgroups and eight *Acanthophrynus* samples from geographically distant localities across the distribution, but not amplified further after establishing the locus was invariant within the ingroup. Sequences, deposited in GenBank (Table 1), were aligned using online MAFFT version 7 (Katoh et al., 2019) with the iterative refinement method G-INS-I, a 200PAM/κ = 2 parameter, and gap opening penalty of 1.53. Outgroup ITS1/2 sequences, too divergent to align unambiguously with *Acanthophrynus*, were omitted from the analyses. The final analyses were based on 148 DNA sequences, with a concatenated alignment length of 6101 bp (Table S5). Alignments are deposited in the Dryad Digital Repository (https://doi.org/10.5061/dryad.z612jm6b8).

2.5 | Phylogenetic analysis

The concatenated multilocus alignment comprised 737 parsimony-informative and 300 singleton sites (Table S6). Whereas the mitochondrial markers were informative for all relationships, the nuclear 28S and 18S markers contained fewer variable sites, informative mostly or only for outgroup relationships, respectively.

Phylogeny estimation with maximum likelihood (ML) was performed using IQ-TREE 2 version 2.0.5 (Minh et al., 2020). The following partitioning schemes and substitution models were selected using MODELFINDER (Kalyaanamoorthy et al., 2017) (-m MF+MERGE) in IQ-TREE 2: 12S + 16S (TIM3+F+G4); 18S + 28S (HKY+F+I); COI first codon position + ITS1/2 (TNe+R2); COI second codon position (TPM2+F+I); COI third codon position (TIM2+F+R2). ML branch support was assessed with 1000 standard nonparametric bootstrap replicates.

MRBAYES version 3.2.7 (Ronquist & Huelsenbeck, 2003) was used for Bayesian inference (BI). Partitioning schemes and substitution models were selected from models available in MRBAYES using IQ-TREE 2 (-m TESTMERGEONLY -mset mrbayes). Only the substitution models differed from the ML analysis, as follows: 12S + 16S (GTR+F+G4), 18S + 28S (HKY+F+I); COI first codon position + ITS1/2 (SYM+I+G4); COI second codon position (F81+F+I); COI third codon position (GTR+F+G4). Two independent runs of MRBAYES, each of four chains with sampling and diagnostic frequencies of 7500 and 75,000, respectively, were performed for 100 million generations on the CIPRES gateway (https://www.phylo.org). Chain convergence was checked using convergence diagnostics, and 25% of the samples were discarded as burn-in, leaving 20,000 trees from which a majority-rule consensus was generated with posterior probabilities reflecting the frequency of samples that recovered each clade.

2.6 | Geographical/genetic barrier analysis

BARRIER version 2.2 (Manni et al., 2004) was used to identify and visualize genetic discontinuities among *Acanthophrynus* populations. Alignments were generated without outgroups using online MAFFT version 7 (Katoh et al., 2019), with the iterative refinement method

TABLE 1 Tissue samples and GenBank accession codes for DNA sequences used for phylogenetic analysis of *Acanthophrynus* whip spiders (Amblypygi). Sequences of mitochondrial 12S rDNA (12S), 16S rDNA (16S), cytochrome *c* oxidase subunit I (COI), and nuclear 18S rDNA (18S), 28S rDNA (28S) and internal transcribed spacer 1 and 2 (ITS1/2) loci. Tissue samples deposited in the Ambrose Monell Collection for Molecular and Microbial Research (AMCC) at the American Museum of Natural History, New York

Species	AMCC	Country: Region: Population	12S	16S	COI	18S	28S	ITS1/2
Acanthophrynus coronatus (Butler, 1873)	LP 5374	Mexico: Sinaloa: SIN 1	MW411546	MW411517	MW410136	MW411506	MW411456	MW411482
	LP 5685	Mexico: Nayarit: NAY 1	MW411547	MW411518	MW410137	MW411507	MW411457	MW411483
	LP 7617	Mexico: Colima: COL 1	MW411548	MW411519	MW410138	MW411508	MW411458	MW411484
	LP 8672	Mexico: Nayarit: NAY 2	MW411549	MW411520	MW410139	MW411509	MW411459	MW411485
	LP 16858	Mexico: Jalisco: JAL 2	MW411550	MW411521	MW410140	—	MW411460	MW411486
	LP 16859	Mexico: Jalisco: JAL 2	MW411551	MW411522	MW410141	—	MW411461	MW411487
	LP 16860	Mexico: Jalisco: JAL 3	MW411552	MW411523	MW410142	MW411510	—	MW411488
	LP 16861	Mexico: Colima: COL 1	MW411553	MW411524	MW410143	MW411511	MW411462	MW411489
	LP 16862	Mexico: Colima: COL 2	MW411554	MW411525	MW410144	—	MW411463	MW411490
	LP 16863	Mexico: Sinaloa: SIN 2	MW411555	MW411526	MW410145	—	—	MW411491
	LP 16864	Mexico: Guerrero: GRO 1	MW411556	MW411527	MW410146	—	MW411464	MW411492
	LP 16865	Mexico: Jalisco: JAL 1	MW411557	MW411528	MW410147	—	MW411465	MW411493
	LP 16866	Mexico: Colima: COL 2	MW411558	MW411529	MW410148	MW411512	MW411466	MW411494
	LP 16869	Mexico: Colima: COL 2	MW411559	MW411530	MW410149	MW411513	MW411467	—
	LP 16881	Mexico: Sinaloa: SIN 1	MW411560	MW411531	MW410150	—	—	MW411495
	LP 16882	Mexico: Michoacán: MIC 2	MW411561	MW411532	MW410151	—	MW411468	—
	LP 16883	Mexico: Michoacán: MIC 3	MW411562	MW411533	MW410152	—	MW411469	MW411496
	LP 16884	Mexico: Guerrero: GRO 2	MW411563	MW411534	MW410153	—	MW411470	MW411497
	LP 16885	Mexico: Morelos: MOR 1	MW411564	MW411535	MW410154	—	MW411471	MW411498
	LP 16886	Mexico: Puebla: PUE 1	MW411565	MW411536	MW410155	—	MW411472	MW411499
	LP 16887	Mexico: Guerrero: GRO 1	MW411566	MW411537	MW410156	—	MW411473	MW411500
	LP 16888	Mexico: Guerrero: GRO 2	MW411567	MW411538	MW410157	—	MW411474	MW411501
	LP 16890	Mexico: Puebla: PUE 1	MW411568	MW411539	MW410158	—	MW411475	MW411502
	LP 16891	Mexico: Colima: COL 1	MW411569	MW411540	MW410159	—	MW411476	MW411503
	LP 16892	Mexico: Michoacán: MIC 1	MW411570	MW411541	MW410160	—	MW411477	MW411504
	LP 16893	Mexico: Jalisco: JAL 2	MW411571	MW411542	MW410161	—	MW411478	MW411505
Heterophrynus longicornis (Butler, 1873)	LP 3830	French Guiana: Approuague-Kaw	MW411572	MW411543	MW410162	MW411514	MW411479	—
Paraphrynus laevifrons (Pocock, 1894)	LP 6145	Costa Rica: Puntarenas	MW411573	MW411544	MW410163	MW411515	MW411480	—
Phrynus marginemaculatus C.L. Koch, 1840	LP 3374	Dom. Rep.: La Altagracia	MW411574	MW411545	MW410164	MW411516	MW411481	—

G-INS-I and a 200PAM/κ = 2 parameter. Alignments are deposited in the Dryad Digital Repository (https://doi.org/10.5061/dryad.z612jm6b8). Mean Kimura 2-parameter (K2P) distances were calculated with all ambiguous positions removed for each sequence pair, among *Acanthophrynus* samples grouped by collection locality for each mitochondrial marker and the nuclear ITS1/2 marker (Tables S7–S10) in MEGA X version 10.1 (Kumar et al., 2018). A separate barrier analysis, computing the first three barriers in decreasing order of intensity, was performed for each marker (Figure S3). A consensus barrier map, integrating information from the different markers, was generated by numbering all barriers identified by at least one marker, counting how many markers identified the barrier, and scoring each barrier recovered per marker with a value of 3, 2 or 1 when recovered as first, second or third barrier, respectively. The relative intensity of each barrier was calculated by dividing the sum of its scores per marker by the highest sum among the barriers.

2.7 | Genetic distances comparison with other whip spiders

Pairwise genetic distances in the 12S, 16S and COI loci of *Acanthophrynus* were compared to intra- and interspecific distances among morphologically distinct but closely related whip spider species of three genera, using data from GenBank: five species of *Damon* C.L. Koch, 1850 from Prendini et al. (2005); three species of *Heterophrynus* Pocock, 1894 from Reveillion et al. (2020); and four species of *Paraphrynus* Moreno, 1940 from Seiter et al. (2020). Sequences were aligned with the *Acanthophrynus* sequences using online MAFFT version 7 (Katoh et al., 2019) with the iterative refinement method G-INS-I and a 200PAM/κ = 2 parameter. Aligned sequences were trimmed to the same length and used to produce one alignment per locus and genus comprising the following number of sequences (*Acanthophrynus* / *Paraphrynus* / *Damon* / *Heterophrynus*): 12S (26/4/13), 16S (24/4/16), COI (23/4/16/63). Alignments are deposited in the Dryad Digital Repository (https://doi.org/10.5061/dryad.z612jm6b8). Single-locus pairwise genetic distances were calculated for each genus in MEGA X using the K2P model (Kimura, 1980) and uniform rates with all ambiguous positions and gaps removed (complete deletion option). K2P distances were averaged across the three mitochondrial loci for each pairwise comparison to identify *Acanthophrynus* clades possibly representing distinct species. The lowest species-level K2P genetic distance was identified among *Damon* species (12.54%) and served as a threshold for identifying *Acanthophrynus* clades in which specimens exhibit higher genetic distances in pairwise comparisons with all specimens outside the respective clade.

2.8 | Divergence dating

The fossil record of whip spiders is sparse (Garwood et al., 2017) and the phylogenetic tree insufficiently resolved to use the few fossils potentially applicable to calibrate the phylogeny of *Acanthophrynus*. Two published clock rates derived from population- or species-level phylogenies of spiders, the closest relatives of whip spiders (Giribet, 2018; Shultz, 2007) for which clock rates are available, were applied: the 16S clock rate of 4% per million years (Myr^{-1}), identified in the mygalomorph spider, *Aptostichus simus* Chamberlin, 1917 (Bond et al., 2001), and commonly used to date the phylogenies of mygalomorph spiders (Kornilios et al., 2016); and a COI clock rate of 10.2% Myr^{-1} derived from the phylogeny of the araneomorph spider, *Dysdera lancerotensis* Simon, 1907 (Bidegaray-Batista et al., 2007). A similar COI rate of 9.8% Myr^{-1} was presented in a species-level phylogeny of other dysderid spiders (Macías-Hernández et al., 2010).

BEAST2 version 2.6.2 (Bouckaert et al., 2019) was used to estimate *Acanthophrynus* divergence times on the topology of the BI tree (Figure 3a), with outgroups removed using the R package APE version 5.4–1 (Paradis et al., 2004). The resulting tree in Newick format was used as starting tree in BEAUTI (Bouckaert et al., 2019) and the operators "narrow exchange," "wide exchange," "Wilson Balding" and "subtree slide" set to zero. Only the aligned mitochondrial sequences for *Acanthophrynus* were used for the BEAST2 analysis. In order to estimate the clock rates of the other loci, each locus was treated as its own partition with the following substitution models selected by MODELFINDER (-m TESTONLY) in IQ-TREE 2: 12S (TN+F+G4); 16S (TN+F+G4); COI (TIM2+F+I+G4); ITS1/2 (TNe+G4). Each partition was assigned an uncorrelated log-normal relaxed molecular clock. In independent runs, the clock rate was either set to 0.02 in 16S or to 0.051 in COI and estimated for the other loci, respectively. A constant coalescent population, recently shown to perform well for phylogenies containing a mix of populations and species (Mello et al., 2021), was selected as tree prior. Markov chain Monte Carlo (MCMC) runs were performed with a chain length of 100 million, sampling every 10,000 generations. The first 10 million generations were discarded as 10% burn-in and the post-burn-in trees used to generate a maximum clade credibility (MCC) tree with mean node heights using TREEANNOTATOR version 2.6.2 (Bouckaert et al., 2019).

2.9 | Ancestral area reconstruction

Ancestral area, vicariance and dispersal event reconstructions were performed using RASP4 version 4.2 (Yu et al., 2015, 2020) on the MCC tree with mean node heights. Six areas were defined, encompassing three ecoregions (i.e., BDDF, JDF and SPDF, and SDF) and reflecting the distribution of *Acanthophrynus* clades recovered in the phylogenetic analysis: Eastern Balsas Dry Forest; Central Balsas Dry Forest; Western Balsas Dry Forest and Southern Jalisco Dry Forest; Northern Jalisco Dry Forest; Southern Sinaloan Dry Forest; and Northern Sinaloan Dry Forest. The maximum range size of the reconstructed ancestral areas was allowed to encompass all six areas. The RASP4-implemented R package BIOGEOBEARS (Matzke, 2013, 2014) was used to select the best-fitting model among six commonly used to reconstruct ancestral geographical distributions: DEC; DIVALIKE; BAYAREALIKE; and the corresponding models including jump dispersal ("+j"). The model selection strongly supported DIVALIKE + j as the best fit to the data.

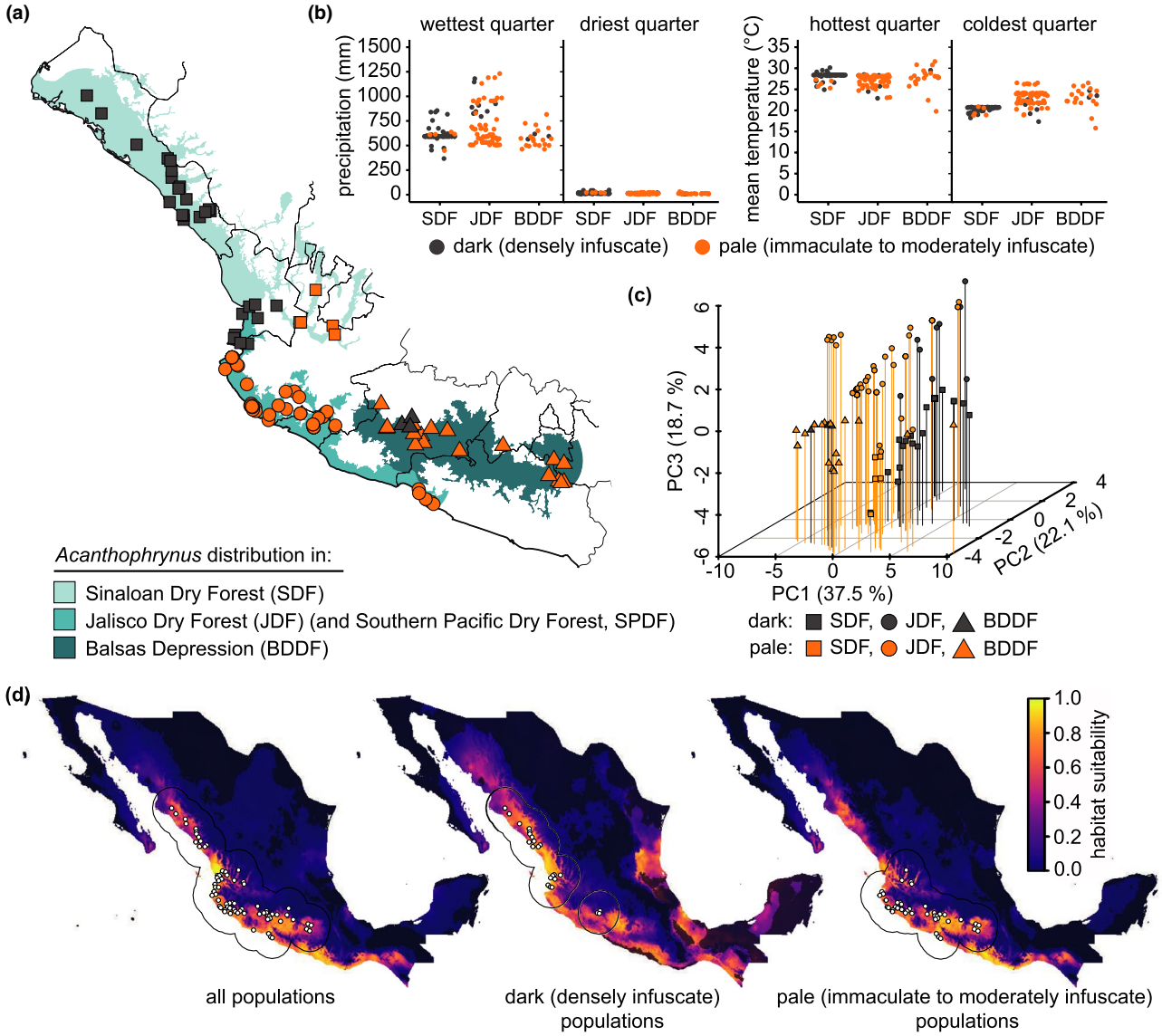

FIGURE 2 Environmental space of *Acanthophrynus* whip spiders (Amblypygi) in Mexican Neotropics. (a) Distribution in Sinaloan Dry Forest (SDF), Jalisco Dry Forest (JDF), including a small part of Southern Pacific Dry Forest (SPDF) in Guerrero, and Balsas Depression Dry Forest (BDDF) with records of dark and pale specimens plotted. Records for which colour could not be determined are not shown. Mexican states abbreviated as follows: COL, Colima; GRO, Guerrero; JAL, Jalisco; MIC, Michoacán; NAY, Nayarit; SIN, Sinaloa. (b) Scatter plots showing total precipitation in wettest/driest 3 months of year and mean temperatures in hottest/coldest 3 months, in ecoregions inhabited by colour variations (a). (c) Three-dimensional scatter plot showing clustering of specimens according to colour and regional provenance based on first, second and third principal components (PC) obtained from 19 hydrothermal bioclimatic covariates. (d) Predicted habitat suitability based on distribution of all populations (all colour variations and those which could not be determined), dark (densely infuscate) populations, and pale (immaculate to moderately infuscate) populations, and environmental layers generated by principal components analysis. Black lines around locality records indicate boundaries of the area from which random background points were sampled. Projections in cloglog output format. Regions with negative multivariate environmental similarity surface values are shaded

3 | RESULTS

3.1 | *Acanthophrynus* distribution

The available records of *Acanthophrynus* are situated in the tropical deciduous forests of the Neotropical Pacific Lowlands and the Balsas Depression biogeographical provinces (Figure 1a). In the Pacific Lowlands, the species is distributed in the SDF Ecoregion, as far north as Sinaloa, the JDF Ecoregion, and the northernmost part of the SPDF Ecoregion, around the city of Zihuatenejo. In the southern parts of the SDF, the species was also recorded where tropical deciduous forest extends into the valleys of the Sierra Madre Occidental.

3.2 | Geographical pattern in colour variation

A distinct geographical pattern was evident in *Acanthophrynus* colour variation (Figure 1; Figure S1). Populations from the BDDF,

JDF, SPDF, and the valleys of the Southern SDF, extending into the Sierra Madre Occidental, varied from orange (immaculate) to dark brown (moderately infuscate) within the same population and among neighbouring populations. For example, all combinations of orange (immaculate) to light brown (sparsely infuscate) pedipalps and light to dark brown (sparsely to moderately infuscate) carapace occur in the vicinity of Chamela, La Huerta, Jalisco (Figure 1b; Figure S1). However, most populations from the coastal regions of Nayarit (JDF) and the SDF were invariant for blackish (densely infuscate) pedipalps and carapace. The boundary between densely infuscate (hereafter, "dark") populations and immaculate to moderately infuscate (hereafter, "pale") populations is situated near the border of the states of Jalisco and Nayarit, where the Sierra Madre del Sur and the Trans-Mexican Volcanic Belt reach the coast, and between the coastal SDF and its extensions into the valleys of the Sierra Madre Occidental (Figure 1a).

3.3 | *Acanthophrynus* environmental space

Acanthophrynus populations experience pronounced seasonality across their distribution, from low precipitation (0–50 mm) in the driest quarter of the year to variable precipitation in the wettest quarter (370–1230 mm) (Figure 2a,b). Dark populations from the northern part of the JDF in Nayarit, and pale populations from the same ecoregion in northern coastal Jalisco (Cabo Corrientes and Tomatlán municipalities) experience higher precipitation (830–1230 mm). Dark populations in the north of the SDF and BDDF, some pale populations in the JDF, and all populations in the BDDF experience lower precipitation. All populations are subject to temperature seasonality with mean temperatures between 25–30°C in the warmest quarter and 20–25°C in the coldest (Figure 2b). The greatest temperature difference between the mean coldest and warmest quarters (8°C) occurs among the dark populations of northern Sinaloa, whereas less seasonality is experienced by populations in other regions.

A PCA of occurrence values for 19 hydrothermal environmental covariates attributed 78% of the variation to the first three principal components (Table S2) and clustered species records in accordance with ecoregion and distance apart (Figure 2c).

3.4 | Environmental niche modelling

Different approaches to environmental niche modelling achieved qualitatively similar results (Figure 2d; Figure S2). Models based on all populations predicted suitable habitat beyond the current distribution in tropical deciduous forests along the Pacific coast of Guerrero (south of Zihuatenejo) and Oaxaca. Whereas the model based on pale populations resulted in similar suitability predictions to the model based on all populations, the model based on dark populations predicted more suitable areas, including the tropical deciduous and evergreen forests of the Atlantic coast and the thorn scrub of coastal Sonora.

High to moderate overlap was observed among predictions based on colour variations, with niche overlap index values (predictions based on PCA environmental layers) of I = 0.78 and D = 0.5, although a niche equivalency test suggested the niches were significantly different ($I_{testmean}$ =0.91 with $p = 1.7 \times 10^{-19}$ and $D_{testmean}$ =0.70 with $p = 1.19 \times 10^{-14}$). A background test, addressing whether niche models were significantly more similar or dissimilar than expected from the respective populations' environmental background achieved different results depending on the direction of comparison. Niche models were significantly more similar when dark populations were compared to the background of the pale populations ($I_{testmean}$ =0.85 with $p = 2.91 \times 10^{-20}$ and $D_{testmean}$ =0.57 with $p = 1.23 \times 10^{-14}$) than vice versa ($I_{testmean}$ =0.64 with $p = 1.7 \times 10^{-35}$ and $D_{testmean}$ =0.31 with $p = 1.39 \times 10^{-39}$). The habitat modelled as preferred by the dark population could be available within the distribution of the pale populations but not vice versa.

3.5 | *Acanthophrynus* phylogeography

Identical tree topologies recovered with BI and ML confirmed the monophyly of *Acanthophrynus* and Phryninae, and placed *Acanthophrynus* in a clade with *Paraphrynus*, to the exclusion of *Phrynus* Lamarck, 1801, with moderate to low support (posterior probability, 0.89; bootstrap support, 0.69) (Figure 3a). Relationships within *Acanthophrynus* received high support. Two major clades were recovered. The "southern clade" comprised pale populations inhabiting parts of the JDF and SPDF ecoregions in eastern Colima and Guerrero, respectively, as well as populations from the BDDF. The "northern clade" comprised dark populations from the northernmost part of the JDF and coastal SDF, and pale populations from the SDF in the southern valleys of the Sierra Madre Occidental and parts of the JDF in Jalisco and western Colima. Although populations in Jalisco and northern Sinaloa formed well-supported clades, their relationship to the sampled populations NAY1 and JAL1 was poorly supported.

3.6 | Mapping *Acanthophrynus* genetic distances

The earliest divergence in the phylogeny does not reflect the geographical distances among the populations comprising the two major clades. The northern and southern clades are situated in close proximity in Colima, ~42 km apart (Figure 3a,b). Several geological features are evident in this region, including the Colima Volcanic Complex, the Colima Rift, and a zone of convergence between the Sierra Madre del Sur and the Trans-Mexican Volcanic Belt (Figure 3c). According to the "barrier analysis," each mitochondrial marker and the nuclear ITS1/2 identified the strongest barrier among *Acanthophrynus* populations in central Colima (Figure 3b; Figure S3). Although divergence in the nuclear 28S locus was too low to calculate multiple barriers, the highest

genetic distances were also among the populations in Colima. The next strongest consensus genetic barriers in decreasing order were between pale populations in the eastern and central, and the central and western Balsas Depression, respectively. These consensus barriers were recovered among populations of the southern clade despite being separated by similar or lower Euclidean distance than some populations of the northern clade. The phylogeny and the barrier analysis suggest lower divergence among the widespread dark populations of the northern clade despite similar or greater geographical distances among them.

Comparison of 12S, 16S and COI genetic distances among *Acanthophrynus* specimens with those at the inter- and intraspecific level in other whip spider genera revealed that the higher end of pairwise genetic distances in *Acanthophrynus* corresponds to the lower end of interspecific distances in other whip spiders (Figure 3d). Averaging across the three mitochondrial loci, the lowest

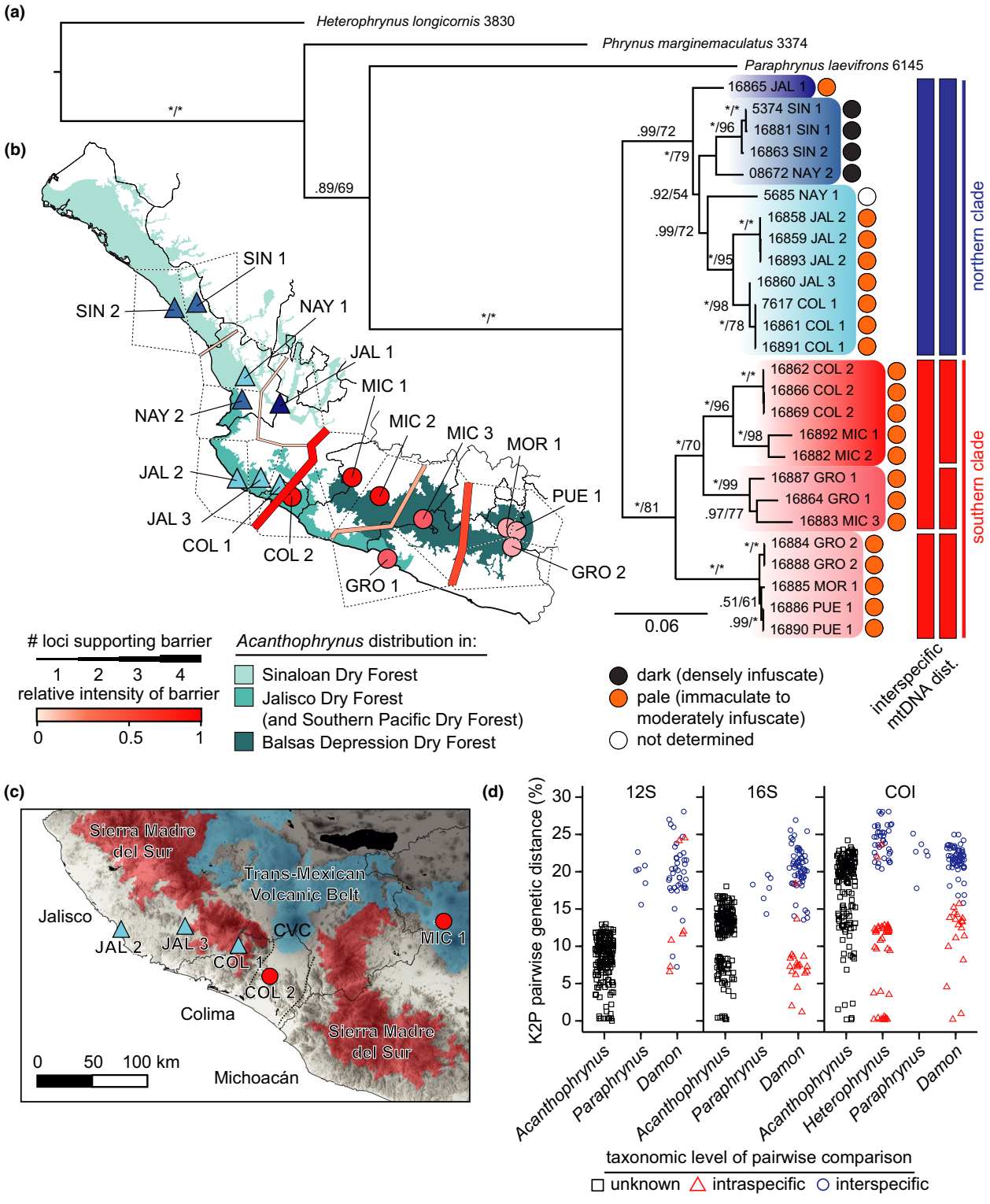

FIGURE 3 Phylogeny and genetic distances of *Acanthophrynus* whip spiders (Amblypygi). (a) Phylogeny estimated with Bayesian inference from concatenated mitochondrial 12S, 16S and COI, and nuclear 18S, 28S and ITS1/2 markers. Major clades are labelled in hues of blue (northern clade) and red (southern clade). Circles adjacent to names indicate colouration: black (dark); orange (pale); white (could not be assessed). Bars adjacent to specimen names indicate potential species-level clades based on Kimura-2-parameter (K2P) pairwise genetic distances averaged over mitochondrial loci (d). First number on branch represents Bayesian posterior probability; second represents corresponding bootstrap support from a topologically identical maximum likelihood tree (asterisks represent maximum probabilities or support, respectively). Ambrose Monell Cryocollection sample numbers correspond to those in Table 1. Mexican states abbreviated as follows: COL, Colima; GRO, Guerrero; JAL, Jalisco; MIC, Michoacán; MOR, Morelos; NAY, Nayarit; PUE, Puebla; SIN, Sinaloa. (b) Map showing locations of populations sampled. Coloured triangles and circles represent populations of northern and southern clades, respectively. Dashed lines indicate Voronoï tessellation map calculated with BARRIER version 2.2. Estimated consensus genetic boundaries based on 12S, 16S, COI and ITS1/2 traced along tessellation map between populations exhibiting highest genetic distances. (c) Coastal region of Jalisco, Colima and Michoacán where populations of northern and southern clades occur in close proximity. Geological features: SMS, Sierra Madre del Sur; TMVB, Trans-Mexican Volcanic Belt; CVC, Colima Volcanic Complex; Colima rift delineated by dashed lines. (d) Scatter plot of pairwise K2P genetic distances in 12S, 16S and COI markers among *Acanthophrynus* and other whip spiders at intra- and interspecific levels

interspecific pairwise distance was among two closely related species, *Damon sylviae* Prendini et al., 2005 and *Damon variegatus* (Perty, 1834) (K2P distance of 12.54%). Using this value as a threshold for interspecific-level divergence in *Acanthophrynus* suggests that the northern clade might represent one species and the southern clade, two or three (Figure 3a).

3.7 | Divergence dating, ancestral area reconstruction and orogeny

Divergence dating based on published molecular clock rates derived from mygalomorph and araneomorph spiders resulted in similar estimates (Figure S4). The earliest divergence among *Acanthophrynus* is estimated to have occurred in the Late Miocene or beginning of the Pliocene, ~6.95 or 5.21 million years ago (Ma), based on the mygalomorph or araneomorph rates, respectively (Figure 4a; Figure S4), when the Sierra Madre Occidental and Sierra Madre del Sur already constituted major geographical barriers. Ancestral area analysis suggests that, prior to the earliest divergence, the common ancestor of *Acanthophrynus* was distributed in a region corresponding to the modern Balsas Depression and Pacific Coast as far as Colima (regions abc in the model), as well as northern Jalisco and Nayarit (e) (Figure 4a,b). The coastal regions of Jalisco (d) and Sinaloa (f) may have been uninhabited, however. The northern and southern clades may have diverged when populations in Nayarit and northern Jalisco (e) became separated from those in the Balsas Depression (abc) by vicariance. A vicariance event around 6.95 or 5.21 Ma falls within the time frame of volcanic activity that gave rise to the Trans-Mexican Volcanic Belt and might have bisected the ancestral range (Figure 4c).

The populations of the eastern Balsas Depression (a) may have separated subsequently (~5.41 or 4.06 Ma, based on the mygalomorph or araneomorph rates, respectively) from other southern clade populations (bc) through vicariance, followed by another vicariance event (~3.91 or 2.93 Ma, based on the mygalomorph or araneomorph rates, respectively) separating populations in the central Balsas Depression (b) from those in the western Balsas Depression and the Pacific Coast as far as Colima (c). The ancestral area reconstruction suggests these vicariance events resulted from the formation of novel barriers, such as habitat fragmentation across the ancestral range of the southern clade. Extant descendants of the northern clade presumably remained restricted to northern Jalisco and Nayarit (e) long after divergence within the southern clade (Figure 4a,b). Thereafter, northern clade populations dispersed into coastal Jalisco and separated from their ancestral distribution by vicariance, ~2.39 or 1.79 Ma, based on the mygalomorph or araneomorph rates, respectively. Sinaloa appears to be the final region to have been colonized by *Acanthophrynus*, into which populations dispersed and then became separated through vicariance, ~1.61 or 1.21 Ma, based on the mygalomorph or araneomorph rates, respectively. The predicted pattern of dispersal followed by vicariance could be consistent with a colonization event across a barrier or the formation of a novel barrier after dispersal.

3.8 | *Acanthophrynus* habitat suitability under past climate scenarios

Areas of suitable habitat for *Acanthophrynus*, predicted for the mid-Holocene (~6 ka), the Last Glacial Maximum (LGM) (~22 ka), and the last interglacial (~140–120 ka) (Figure 5a,b) were largely in agreement under different general circulation models and modeling approaches (Figures S5 and S6). Whereas the suitable habitat predicted in Mexico during the mid-Holocene resembles present-day predictions, it was significantly reduced during the LGM, being concentrated in Nayarit, the ancestral area hypothesized for the northern clade (Figure 4b,c). Sinaloa and, to a lesser extent, Jalisco, into which the northern clade is hypothesized to have dispersed later, contained significantly less suitable habitat. Suitable habitat was also reduced in the Balsas Depression. Although the mean temperatures of the hottest and coldest months dropped throughout the distribution of *Acanthophrynus* during the LGM, the lowest temperatures were in Sinaloa (Figure 5c), where the mean temperature of the coldest quarter may have dropped to 13–15°C, far below the usual temperatures of areas inhabited by *Acanthophrynus* today.

All regions probably also received less precipitation during the LGM, with the Balsas Depression especially affected. During the last interglacial, suitable habitat is predicted to have been concentrated

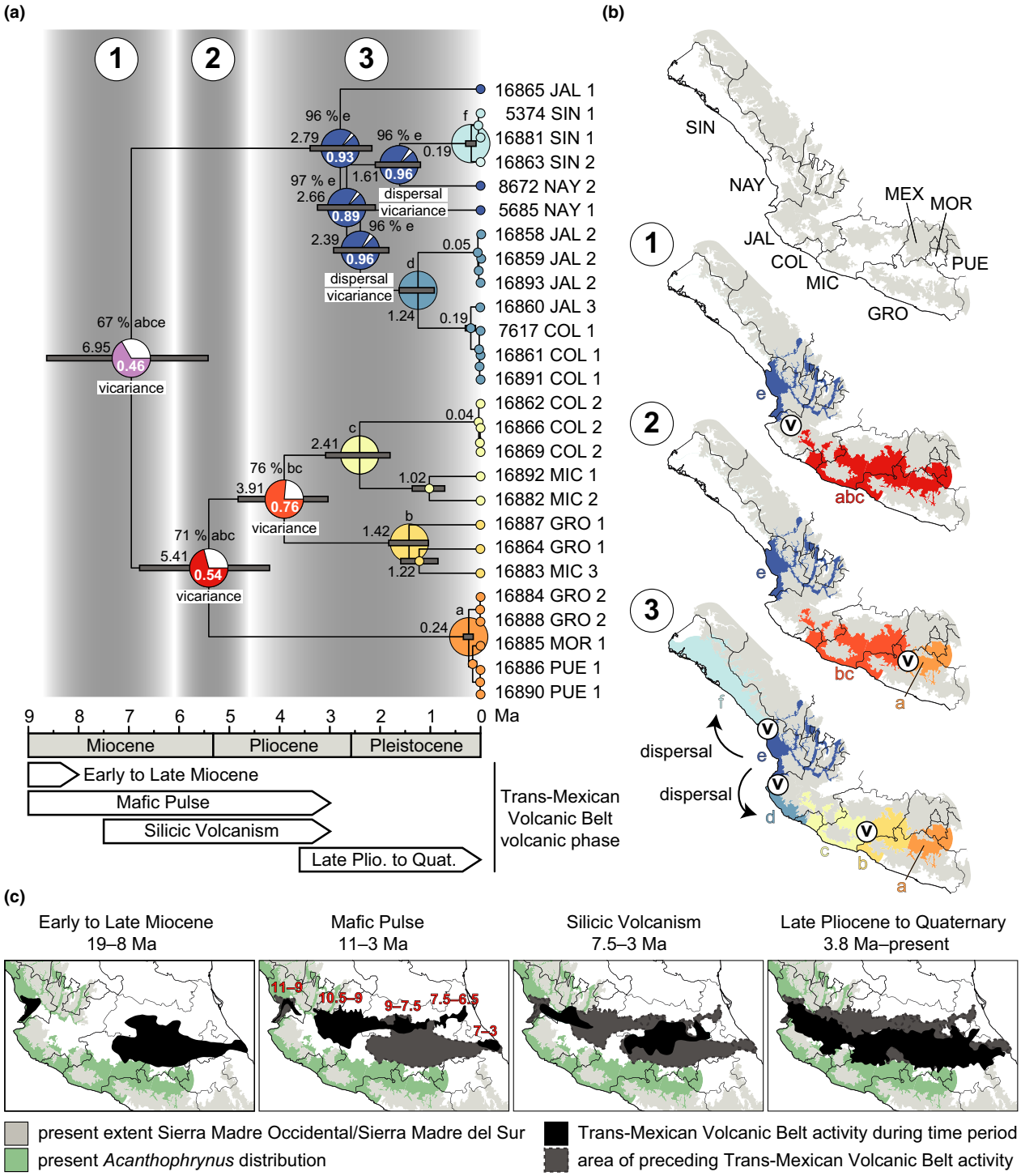

FIGURE 4 Divergence dating and ancestral area reconstruction in *Acanthophrynus* whip spiders (Amblypygi). (a) Mygalomorph clock rate-calibrated phylogeny estimated in BEAST2 with geological time frames beneath the tree. Numbers left of nodes indicate median age estimates. Grey bars at nodes represent 95% highest posterior density (HPD) around age estimates. Pie charts on nodes represent the probability of reconstructed ancestral areas (b) estimated according to the DIVALIKE + j biogeographical model in RASP4. Only areas with probabilities >15% are shown in charts, extent and probability of ancestral areas indicated above nodes (combinations of present-day areas a–f). Event probabilities associated with nodes are in white inside pie charts. Predicted vicariance and dispersal events are indicated on respective nodes. Time frame of events (b) numbered and highlighted in grey. Ambrose Monell Cryocollection sample numbers correspond to those in Table 1. Mexican states abbreviated as follows: COL, Colima; GRO, Guerrero; JAL, Jalisco; MIC, Michoacán; MOR, Morelos; NAY, Nayarit; PUE, Puebla; SIN, Sinaloa. (b) Panels presenting potential ancestral distribution during time frame (a). Areas based on present distribution of species and reflect major clades recovered in the phylogeny. Vicariance events (v) are indicated at boundary of regions, and dispersal events and direction thereof, as arrows. Current extent of mountain ranges in grey. (c) Panels showing time frames and geographical extent of four magmatic episodes of the Trans-Mexican Volcanic Belt in relation to present distribution (after Ferrari et al., 2012)

in Nayarit, but Sinaloa may also have been habitable, as temperature and precipitation ranges resemble contemporary conditions (Figure 5b,c). Less suitable habitat was present in the Balsas Depression during the last interglacial, however, in which mean temperatures for the hottest quarter were highest among the three reconstructed time periods.

4 | DISCUSSION

4.1 | Cryptic diversification decoupled from ecological adaption and phenotypic change

The distribution of *Acanthophrynus*, which spans three biogeographical regions, is unusually wide for a whip spider species. The distributions of most whip spider species, especially among the closely related phrynid genera, *Paraphrynus* and *Phrynus*, are far more restricted (Armas, 2006; Seiter et al., 2020). For example, only two of 18 morphologically delimited species of *Paraphrynus* in Mexico occur in more than one biogeographical region (Ballesteros, 2010). Eight morphologically and genetically delimited species of the tarantula genus *Brachypelma* Simon, 1891 occur across the distribution of *Acanthophrynus* (Mendoza & Francke, 2020). Recent genetic studies on phrynid whip spiders of the genera *Heterophrynus* and *Phrynus* suggested large pairwise genetic distances may reflect previously unrecognized cryptic diversity (Esposito et al., 2015; Reveillion et al., 2020). Pairwise genetic distances within *Acanthophrynus* resemble intra- and interspecific distances among morphologically diagnosable whip spider species of other genera, suggesting the monotypic *Acanthophrynus* is a complex of three or four cryptic species.

In the present study, several colour variations were observed and a pattern was evident in the geographical distributions of the pale (immaculate to moderately infuscate) and dark (densely infuscate) populations. Although closely related to the pale populations, the dark populations of the SDF Ecoregion formed a separate clade. Colouration is an important character in the species delimitation and diagnosis of *Brachypelma* tarantulas (Mendoza & Francke, 2020), codistributed with *Acanthophrynus*. The geographical boundary between two distinctly coloured *Brachypelma* species, near the border between the states of Jalisco and Nayarit, resembles the boundary between the dark and pale populations of *Acanthophrynus*. Colouration may prove informative for the taxonomy of *Acanthophrynus*, and may coincide with other, less obvious differences.

The environmental niche models presented here predict differences among the niches occupied by populations of *Acanthophrynus* with different colouration. However, the PCA suggests that populations with different colouration cluster due to the environmental conditions of different geographical regions rather than due to similarity in colouration (Figure 2c). For example, three dark populations cluster with pale populations in the BDDF.

The deepest divergence in the phylogeny of *Acanthophrynus*, reflecting the species level in morphologically distinct whip spiders of other genera, is observed among phenotypically similar populations inhabiting similar environments in geographical proximity in Colima and the central and eastern Balsas Depression. These data suggest species-level diversification in *Acanthophrynus* was decoupled from ecological adaptation and phenotypic variation. Although often driven by adaptation and niche divergence, as exemplified by adaptive radiation (Gillespie, 2004; Irisarri et al., 2018; Losos et al., 1998), diversification in the tropics commonly results from a combination of factors, many of which may be nonadaptive (Rundell & Price, 2009). Much tropical diversity may be the product of repeated allopatric speciation driven by vicariance and dispersal in a heterogeneous landscape and in association with a temporally fluctuating climate (Simões et al., 2016). As cryptic diversity becomes better understood, across a broader array of taxa, more examples in which diversification was driven by such nonadaptive factors are likely to be revealed.

4.2 | Landscape modification as a driver of diversification in the tropics

The geographical boundaries of the major clades of *Acanthophrynus* bear little resemblance to the Neotropical biogeographical provinces of Mexico or the ecoregions nested within them. A marked disconnect between genetic and geographical distances is evident in Colima, located centrally in the JDF Ecoregion and the larger Pacific Lowlands Province, where populations of the northern and southern clades occur in close geographical proximity, only ~42 km apart. Similar geographical boundaries have been observed among other Neotropical taxa in the Pacific Lowlands, including reptiles, fish and tarantulas (Mateos et al., 2002; Mendoza & Francke, 2020; Suárez-Atilano et al., 2014; Zarza et al., 2008). The emergence of geographical features such as the Trans-Mexican Volcanic Belt in Colima has been suggested to have driven divergence in *Boa constrictor imperator* Daudin, 1803 and the iguana *Ctenosaura pectinata* Wiegmann, 1834 (Suárez-Atilano et al., 2014; Zarza et al., 2008) although later studies suggested the genetic boundary in *C. pectinata* does not reflect a physical barrier, as interbreeding occurs among geographically adjacent clades (Zarza et al., 2011, 2019). The ancestral area reconstruction suggests divergence between the two clades of *Acanthophrynus* occurred elsewhere and populations came into proximity in Colima later, as in *C. pectinata*. It is unknown whether geological features in Colima impose a physical barrier to *Acanthophrynus* or whether geographically adjacent populations come into contact. Given the high genetic distances between the two clades of *Acanthophrynus*, corresponding to interspecific distances in other whip spiders, and the presence of a boundary between two species of *Brachypelma* tarantulas in the same area (Mendoza & Francke, 2020), Colima may constitute a boundary between two cryptic species of *Acanthophrynus*.

It is difficult to determine whether similar boundaries observed in different taxa reflect the same or different biogeographical events. *Acanthophrynus* divergence into the two clades in Colima, estimated at ~6.95 or 5.21 Ma, based on the mygalomorph and araneomorph

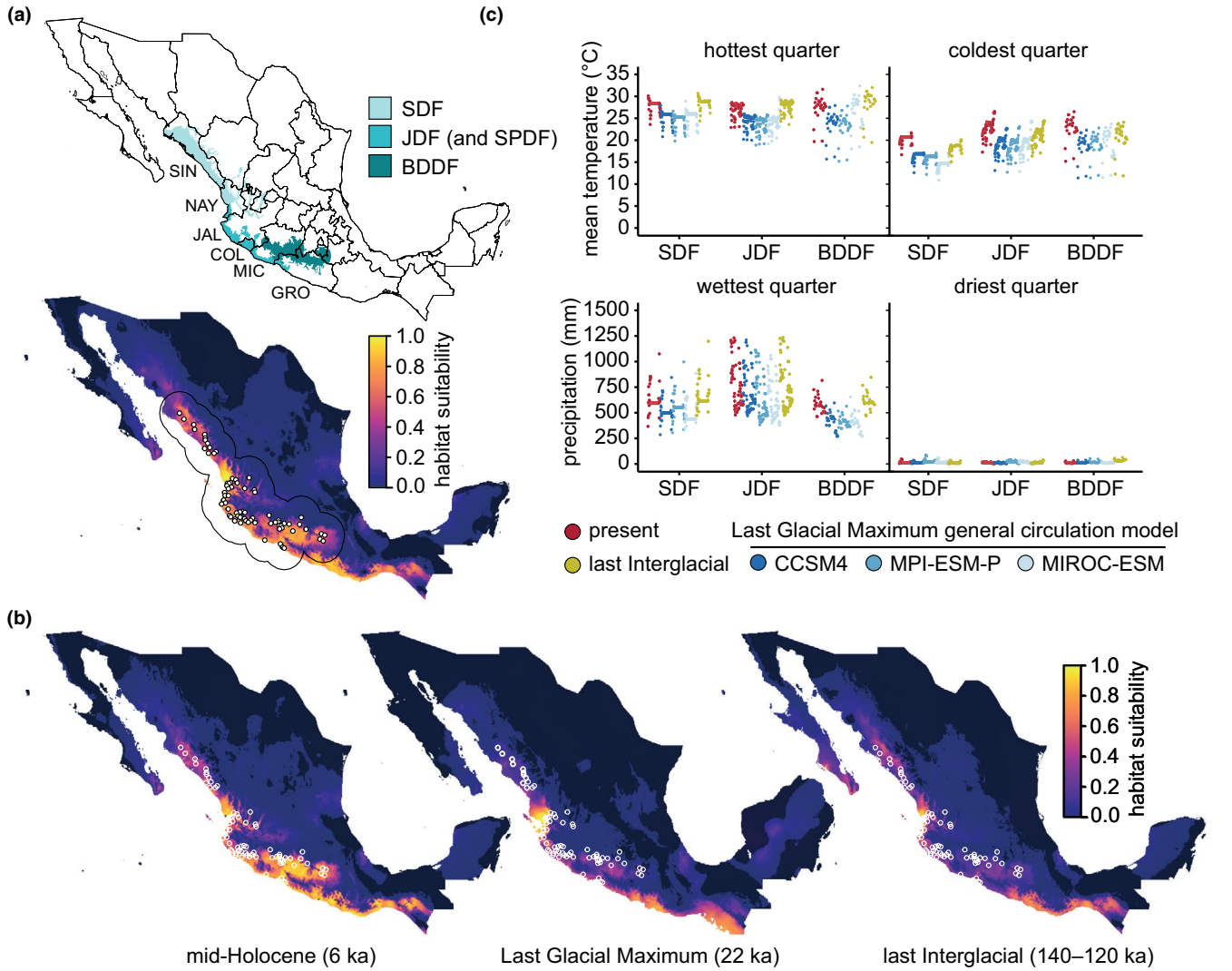

FIGURE 5 Predictions of habitat suitability for *Acanthophrynus* whip spiders (Amblypygi) during the last glacial/interglacial cycle. (a) Present distribution and predicted habitat suitability based on principal components analysis-generated environmental layers using the distribution of all populations (as in Figure 2d). (b) Predicted habitat suitability during the mid-Holocene (CCSM4 model), Last Glacial Maximum (CCSM4 model) and last interglacial. Projections in cloglog output format. Regions with negative multivariate environmental similarity surfaces values shaded. Hollow circles denote present-day records. (c) Scatter plots showing total precipitation in the wettest/driest 3 months of year and mean temperatures in the hottest/coldest 3 months at localities corresponding to present-day records during past climate scenarios. Records are subdivided by biogeographical provinces

rates, respectively, may have been driven by the same events responsible for the earliest divergence in *C. pectinata* iguanas, around 6.5–2.3 Ma. The Mafic Pulse and Silicic Volcanism phases (11–3 Ma) of the Trans-Mexican Volcanic Belt orogeny, which occurred in the ancestral range of *Acanthophrynus*, probably drove divergence by vicariance and formed a lasting barrier throughout the remainder of its history. Although the northern clade may have originated from a dispersal event across the nascent Trans-Mexican Volcanic Belt, the data suggest it was probably already present to the north, and divergence was driven by vicariance as the mountain range emerged.

Observations of differing divergence times in different taxa have led to debate about the role of landscape modification, such as orogeny, in driving tropical diversification (Garzón-Orduña et al., 2014; Hoorn et al., 2010; Rull, 2008, 2011; Smith et al., 2014). The sensitivity or proclivity of taxa to vicariance, due to intrinsic biological characteristics such as vagility or ecological specialization (stenotopy vs. eurytopy), is likely to affect if and when landscape changes will constitute an effective barrier. A large-scale study on the diversification of Amazonian birds demonstrated that diversification is driven by an interplay between landscape evolution and the age, persistence and vagility of a lineage in a region (Smith et al., 2014).

4.3 | Palaeoclimatic change modulating diversification in the tropics

Past climate projections presented herein suggest that glacial/interglacial cycles which commenced in the late Pliocene (~3 Ma)

probably caused repeated range expansion and contraction in *Acanthophrynus*. Whereas the molecular dating suggests divergence in the southern clade began prior to the Pliocene, perhaps in association with the development of the Balsas River (Mendoza & Francke, 2017), habitat fragmentation in the Balsas Depression could account for later divergence, as the extent of suitable habitat reduced during the LGM and the last interglacial. In contrast, the models suggest the northern clade may have been largely confined to parts of Nayarit during glacial periods. Sinaloa, in particular, appears to have been largely uninhabitable during the LGM, consistent with the low genetic divergence among populations of the northern clade, and the ancestral area reconstruction of a late southward dispersal into Jalisco and Colima, followed by a northward dispersal into Sinaloa. Areas predicted to be uninhabitable during the LGM, such as Sinaloa, may have been inhabited by earlier lineages during previous interglacials, and subsequently replaced.

The different timing of divergence observed in the northern and southern clades of *Acanthophrynus* suggest that, whereas climatic fluctuations may have driven further diversification in the Balsas Depression, the more severe fluctuations in the northern part of the distribution may have hindered dispersal and/or resulted in extinction, ultimately limiting the spatiotemporal opportunity for diversification. The relatively broad distributions of populations belonging to the same clade or species of other codistributed vertebrate and arthropod taxa in the SDF Ecoregion suggest that later diversification in the north is a general pattern (Mendoza & Francke, 2020; Suárez-Atilano et al., 2014; Zarza et al., 2008). Remarkably, this pattern mirrors the latitudinal gradient of biodiversity, according to which differential spatiotemporal opportunity between tropical and temperate biomes accounts for increased biodiversity in the tropics (Fine & Ree, 2006; Wiens & Donoghue, 2004).

5 | CONCLUSION

The present study addressed the roles of landscape and palaeoclimatic change in driving tropical diversification using a model system, the whip spider, *Acanthophrynus*, widespread in the tropical deciduous forests of Mexico. The results revealed, first, that although morphological and environmental variation may be apparent across the distribution of an organism, this variation does not necessarily reflect major diversification events. Instead, much of the diversification might be cryptic and decoupled from environmental adaptation. Diversification may primarily be a product of the repeated appearance and disappearance of barriers as habitat mosaics fragment and coalesce across a topographically complex landscape, in response to a changing climate. Second, the extent to which major geographical barriers, such as the Trans-Mexican Volcanic Belt, drive diversification probably depends on the intrinsic biological characteristics of taxa, such as vagility and ecological specialization. Arthropods with stenotopic ecological requirements and/or limited vagility may undergo a higher rate of speciation than codistributed vertebrates. Finally, palaeoclimatic fluctuations may act both as drivers and inhibitors of diversification across the distribution of a taxon. Whereas diversification may be driven by climate-induced habitat fragmentation in one area, reduction in the extent of suitable habitat might reduce the spatiotemporal opportunity for diversification in another.

ACKNOWLEDGMENTS

F.D.S. was supported by a short-term research scholarship by the German Academic Exchange Service (Deutscher Akademischer Austauschdienst, DAAD). Fieldwork was supported by a grant to F.D.S. from the Theodore Roosevelt Memorial Fund of the AMNH, and grants to A.V.-M. from the Consejo Nacional de Ciencia y Tecnología (CONACyT), Mexico, and the Laboratorio Regional de Biodiversidad y Cultivo de Tejidos Vegetales del Instituto Biología, Universidad Nacional Autónoma de México, sede Tlaxcala. DNA sequencing at the AMNH was supported by National Science Foundation DEB 2003382 grant to L.P. Material was collected under Scientific Collector Permit FAUT-0309 from the Secretaría de Medio Ambiente y Recursos Naturales (SEMARNAT), Mexico, to A.V.-M. The authors thank Oscar F. Francke (CNAN), Lauren Esposito and Darrel Ubick (CAS), Christoph Hörweg and Michael Seiter (NHMW), Hannah Wood and Dana DeRoche (USNM), Danilo Harms (ZMH) and Janet Beccaloni (BMNH) for the loans of material; Oscar F. Francke (CNAN) for permitting tissue dissections; Pío Colmenares for logistical assistance at the AMNH; Michael Seiter, Iker Irisarri and Stephanie Loria for advice and comments on the manuscript; LATLAX students for assistance in the field and processing material; Marina Mejía-Duque, Dulce Vivar and Diego Barrales-Alcalá for providing photographs; and Rosemary Gillespie, Ingi Agnarsson and two anonymous reviewers for constructive criticism which greatly improved the manuscript.

AUTHOR CONTRIBUTIONS

F.D.S. and L.P. conceived the study. A.V.-M. contributed material used in the study. F.D.S. processed the data, conducted the analyses and designed the figures. F.D.S., A.V.-M. and L.P. interpreted results. F.D.S. and L.P. wrote the manuscript commented on by A.V.-M. F.D.S., A.V.-M. and L.P. acquired funding for the study.

DATA AVAILABILITY STATEMENT

All data supporting the findings of this study are openly accessible. DNA sequences are deposited in GenBank (https://www.ncbi.nlm.nih.gov/genbank) under accession nos. MW410136–MW410164 and MW411456–MW411574. Raw and processed data, and R scripts used for the analysis and plotting, are deposited in the Dryad Digital Repository (https://www.datadryad.org): https://doi.org/10.5061/dryad.z612jm6b8 (Schramm et al., 2021).

ORCID

Frederic D. Schramm https://orcid.org/0000-0003-1858-7770
Alejandro Valdez-Mondragón https://orcid.org/0000-0001-5385-3195
Lorenzo Prendini https://orcid.org/0000-0001-8727-7106

REFERENCES

Aiello-Lammens, M. E., Boria, R. A., Radosavljevic, A., Vilela, B., & Anderson, R. P. (2015). spThin: An R package for spatial thinning of species occurrence records for use in ecological niche models. *Ecography*, *38*(5), 541–545. https://doi.org/10.1111/ecog.01132

Armas, L. F. (2006). Los amblipígidos o tendarapos de México (Arachnida: Amblypygi). *Boletín Sociedad Entomológica Aragonesa*, *39*, 345–359.

Ballesteros, J. A. (2010). *Sistemática filogenética del género* Paraphrynus *Moreno (Arachnida: Amblypygi: Phrynidae)* (Unpublished Master's thesis). Universidad Nacional Autónoma de México, Mexico City.

Bidegaray-Batista, L., Macías-Hernández, N., Oromí, P., & Arnedo, M. A. (2007). Living on the edge: Demographic and phylogeographical patterns in the woodlouse-hunter spider *Dysdera lancerotensis* Simon, 1907 on the eastern volcanic ridge of the Canary Islands. *Molecular Ecology*, *16*(15), 3198–3214. https://doi.org/10.1111/j.1365-294X.2007.03351.x

Bond, J. E., Hedin, M. C., Ramírez, M. G., & Opell, B. D. (2001). Deep molecular divergence in the absence of morphological and ecological change in the Californian coastal dune endemic trapdoor spider *Aptostichus simus*. *Molecular Ecology*, *10*(4), 899–910. https://doi.org/10.1046/j.1365-294X.2001.01233.x

Bouckaert, R., Vaughan, T. G., Barido-Sottani, J., Duchêne, S., Fourment, M., Gavryushkina, A., Heled, J., Jones, G., Kühnert, D., De Maio, N., Matschiner, M., Mendes, F. K., Müller, N. F., Ogilvie, H. A., du Plessis, L., Popinga, A., Rambaut, A., Rasmussen, D., Siveroni, I., … Drummond, A. J. (2019). BEAST 2.5: An advanced software platform for Bayesian evolutionary analysis. *PLoS Computational Biology*, *15*(4), e1006650. https://doi.org/10.1371/journal.pcbi.1006650

Bryson, R. W., García-Vázquez, U. O., & Riddle, B. R. (2011). Phylogeography of Middle American gophersnakes: Mixed responses to biogeographical barriers across the Mexican Transition Zone. *Journal of Biogeography*, *38*(8), 1570–1584. https://doi.org/10.1111/j.1365-2699.2011.02508.x

Chapin, K. J., Winkler, D. E., Wiencek, P., & Agnarsson, I. (2018). Island biogeography and ecological modeling of the amblypygid *Phrynus marginemaculatus* in the Florida Keys archipelago. *Ecology and Evolution*, *8*(18), 9139–9151. https://doi.org/10.1002/ece3.4333

Clouse, R. M., Sharma, P. P., Stuart, J. C., Davis, L. R., Giribet, G., Boyer, S. L., & Wheeler, W. C. (2016). Phylogeography of the harvestman genus *Metasiro* (Arthropoda, Arachnida, Opiliones) reveals a potential solution to the Pangean paradox. *Organisms, Diversity and Evolution*, *16*(1), 167–184. https://doi.org/10.1007/s13127-015-0233-7

Elith, J., Kearney, M., & Phillips, S. (2010). The art of modelling range-shifting species. *Methods in Ecology and Evolution*, *1*(4), 330–342. https://doi.org/10.1111/j.2041-210x.2010.00036.x

Esposito, L. A., Bloom, T., Caicedo-Quiroga, L., Alicea-Serrano, A. M., Sánchez-Ruíz, J. A., May-Collado, L. J., Binford, G. J., & Agnarsson, I. (2015). Islands within islands: Diversification of tailless whip spiders (Amblypygi, *Phrynus*) in Caribbean caves. *Molecular Phylogenetics and Evolution*, *93*, 107–117. https://doi.org/10.1016/j.ympev.2015.07.005

Farr, T. G., Rosen, P. A., Caro, E., Crippen, R., Duren, R., Hensley, S., Kobrick, M., Paller, M., Rodriguez, E., Roth, L., Seal, D., Shaffer, S., Shimada, J., Umland, J., Werner, M., Oskin, M., Burbank, D., & Alsdorf, D. (2007). The shuttle radar topography mission. *Reviews of Geophysics*, *45*(2), RG2004. https://doi.org/10.1029/2005RG000183.1.INTRODUCTION

Ferrari, L., Orozco-Esquivel, T., Manea, V., & Manea, M. (2012). The dynamic history of the Trans-Mexican Volcanic Belt and the Mexico subduction zone. *Tectonophysics*, *522–523*, 122–149. https://doi.org/10.1016/j.tecto.2011.09.018

Ferrier, S., Gray, M. R., Cassis, G. A., & Wilkie, L. (1999). Spatial turnover in species composition of ground-dwelling arthropods, vertebrates and vascular plants in north-east New South Wales: Implications for selection of forest reserves. In W. Ponder, & D. Lunney (Eds.), *The other 99%: The conservation and biodiversity of invertebrates* (pp. 68–76). Royal Zoological Society of New South Wales. https://doi.org/10.7882/rzsnsw.1999.013

Fick, S. E., & Hijmans, R. J. (2017). WorldClim 2: New 1-km spatial resolution climate surfaces for global land areas. *International Journal of Climatology*, *37*(12), 4302–4315. https://doi.org/10.1002/joc.5086

Fine, P. V. A. (2015). Ecological and evolutionary drivers of geographic variation in species diversity. *Annual Review of Ecology, Evolution, and Systematics*, *46*, 369–392. https://doi.org/10.1146/annurev-ecolsys-112414-054102

Fine, P. V. A., & Ree, R. H. (2006). Evidence for a time-integrated species-area effect on the latitudinal gradient in tree diversity. *American Naturalist*, *168*(6), 796–804. https://doi.org/10.1086/508635

Garwood, R. J., Dunlop, J. A., Knecht, B. J., & Hegna, T. A. (2017). The phylogeny of fossil whip spiders. *BMC Evolutionary Biology*, *17*, 105. https://doi.org/10.1186/s12862-017-0931-1

Garzón-Orduña, I. J., Benetti-Longhini, J. E., & Brower, A. V. Z. (2014). Timing the diversification of the Amazonian biota: Butterfly divergences are consistent with Pleistocene refugia. *Journal of Biogeography*, *41*(9), 1631–1638. https://doi.org/10.1111/jbi.12330

Gent, P. R., Danabasoglu, G., Donner, L. J., Holland, M. M., Hunke, E. C., Jayne, S. R., Lawrence, D. M., Neale, R. B., Rasch, P. J., Vertenstein, M., Worley, P. H., Yang, Z.-L., & Zhang, M. (2011). The community climate system model version 4. *Journal of Climate*, *24*(19), 4973–4991. https://doi.org/10.1175/2011JCLI4083.1

Gentry, A. H. (1995). Diversity and floristic composition of neotropical dry forests. In S. Bullock, H. Mooney, & E. Medina (Eds.), *Seasonally dry tropical forests* (pp. 146–194). Cambridge University Press. https://doi.org/10.1017/cbo9780511753398.007

Ghalambor, C. K. (2006). Are mountain passes higher in the tropics? Janzen's hypothesis revisited. *Integrative and Comparative Biology*, *46*(1), 5–17. https://doi.org/10.1093/icb/icj003

Gillespie, R. G. (2004). Community assembly through adaptive radiation in Hawaiian spiders. *Science*, *303*, 356–359.

Gillespie, R. G., Bennett, G. M., De Meester, L., Feder, J. L., Fleischer, R. C., Harmon, L. J., Hendry, A. P., Knope, M. L., Mallet, J., Martin, C., Parent, C. E., Patton, A. H., Pfennig, K. S., Rubinoff, D., Schluter, D., Seehausen, O., Shaw, K. L., Stacy, E., Stervander, M., … Wogan, G. O. U. (2020). Comparing adaptive radiations across space, time, and taxa. *Journal of Heredity*, *111*(1), 1–20. https://doi.org/10.1093/jhered/esz064

Giribet, G. (2018). Current views on chelicerate phylogeny—A tribute to Peter Weygoldt. *Zoologischer Anzeiger*, *273*, 7–13. https://doi.org/10.1016/j.jcz.2018.01.004

Halffter, G., & Morrone, J. J. (2017). An analytical review of Halffter's Mexican transition zone, and its relevance for evolutionary biogeography, ecology and biogeographical regionalization. *Zootaxa*, *4226*(1), 1–46. https://doi.org/10.11646/zootaxa.4226.1.1

Harrison, S. E., Harvey, M. S., Cooper, S. J. B., Austin, A. D., & Rix, M. G. (2017). Across the Indian Ocean: A remarkable example of trans-oceanic dispersal in an austral mygalomorph spider. *PLoS One*, *12*(8), e0180139. https://doi.org/10.1371/journal.pone.0180139

Harvey, M. S. (2003). Order Amblypygi Thorell. In *Catalogue of the smaller arachnid orders of the World: Amblypygi, Uropygi, Schizomida, Palpigradi, Ricinulei and Solifugae* (pp. 1–58). CSIRO Publishing.

Hijmans, R. J., Cameron, S. E., Parra, J. L., Jones, P. G., & Jarvis, A. (2005). Very high resolution interpolated climate surfaces for global land areas. *International Journal of Climatology*, *25*(15), 1965–1978. https://doi.org/10.1002/joc.1276

Hijmans, R. J., Philips, S., Leathwick, J., & Elith, J. (2020). *dismo: Species distribution modeling*. R package version 1.3–3. https://doi.org/10.1016/b978-0-12-809633-8.02390-6

Hijmans, R. J., & Van Etten, J. (2020). *raster: Geographic analysis and modeling with raster data*. R package version 3.4-5. https://cran.r-project.org/package=raster

Hoorn, C., Wesselingh, F. P., ter Steege, H., Bermudez, M. A., Mora, A., Sevink, J., Sanmartin, I., Sanchez-Meseguer, A., Anderson, C. L., Figueiredo, J. P., Jaramillo, C., Riff, D., Negri, F. R., Hooghiemstra, H., Lundberg, J., Stadler, T., Sarkinen, T., & Antonelli, A. (2010). Amazonia through time: Andean uplift, climate change, landscape evolution, and biodiversity. *Science*, *330*(6006), 927–931. https://doi.org/10.1126/science.1194585

Irisarri, I., Singh, P., Koblmüller, S., Torres-Dowdall, J., Henning, F., Franchini, P., Fischer, C., Lemmon, A. R., Lemmon, E. M., Thallinger, G. G., Sturmbauer, C., & Meyer, A. (2018). Phylogenomics uncovers early hybridization and adaptive loci shaping the radiation of Lake Tanganyika cichlid fishes. *Nature Communications*, *9*, 3159. https://doi.org/10.1038/s41467-018-05479-9

Janzen, D. H. (1967). Why mountain passes are higher in the tropics. *The American Naturalist*, *101*(919), 233–249. https://doi.org/10.1086/282487

K-1 Model Developers. (2004). K-1 coupled GCM (MIROC) description. In *K-1 Technical Report*. Center for Climate System Research, University of Tokyo.

Kalyaanamoorthy, S., Minh, B. Q., Wong, T. K. F., Von Haeseler, A., & Jermiin, L. S. (2017). ModelFinder: Fast model selection for accurate phylogenetic estimates. *Nature Methods*, *14*(6), 587–589. https://doi.org/10.1038/nmeth.4285

Kass, J. M., Vilela, B., Aiello-Lammens, M. E., Muscarella, R., Merow, C., & Anderson, R. P. (2018). Wallace: A flexible platform for reproducible modeling of species niches and distributions built for community expansion. *Methods in Ecology and Evolution*, *9*(4), 1151–1156. https://doi.org/10.1111/2041-210X.12945

Katoh, K., Rozewicki, J., & Yamada, K. D. (2019). MAFFT online service: Multiple sequence alignment, interactive sequence choice and visualization. *Briefings in Bioinformatics*, *20*(4), 1160–1166. https://doi.org/10.1093/bib/bbx108

Kimura, M. (1980). A simple method for estimating evolutionary rates of base substitutions through comparative studies of nucleotide sequences. *Journal of Molecular Evolution*, *16*(2), 111–120. https://doi.org/10.1007/BF01731581

Kornilios, P., Thanou, E., Kapli, P., Parmakelis, A., & Chatzaki, M. (2016). Peeking through the trapdoor: Historical biogeography of the Aegean endemic spider *Cyrtocarenum* Ausserer, 1871 with an estimation of mtDNA substitution rates for Mygalomorphae. *Molecular Phylogenetics and Evolution*, *98*, 300–313. https://doi.org/10.1016/j.ympev.2016.01.021

Kumar, S., Stecher, G., Li, M., Knyaz, C., & Tamura, K. (2018). MEGA X: Molecular evolutionary genetics analysis across computing platforms. *Molecular Biology and Evolution*, *35*(6), 1547–1549. https://doi.org/10.1093/molbev/msy096

Loria, S. F., & Prendini, L. (2020). Out of India, thrice: Diversification of Asian forest scorpions reveals three colonizations of Southeast Asia. *Scientific Reports*, *10*(1), 1–19. https://doi.org/10.1038/s41598-020-78183-8

Losos, J. B., Jackman, T. R., Larson, A., de Queiroz, K., & Rodríguez-Schettino, L. (1998). Contingency and determinism in replicated adaptive radiations of island lizards. *Science*, *279*, 2115–2118.

Macías-Hernández, N., Oromí, P., & Arnedo, M. A. (2010). Integrative taxonomy uncovers hidden species diversity in woodlouse hunter spiders (Araneae, Dysderidae) endemic to the Macaronesian archipelagos. *Systematics and Biodiversity*, *8*(4), 531–553. https://doi.org/10.1080/14772000.2010.535865

Manni, F., Guérard, E., & Heyer, E. (2004). Geographic patterns of (genetic, morphologic, linguistic) variation: How barriers can be detected by using Monmonier's algorithm. *Human Biology*, *76*(2), 173–190. https://doi.org/10.1353/hub.2004.0034

Mastretta-Yanes, A., Moreno-Letelier, A., Piñero, D., Jorgensen, T. H., & Emerson, B. C. (2015). Biodiversity in the Mexican highlands and the interaction of geology, geography and climate within the Trans-Mexican Volcanic Belt. *Journal of Biogeography*, *42*(9), 1586–1600. https://doi.org/10.1111/jbi.12546

Mateos, M., Sanjur, O. I., & Vrijenhoek, R. C. (2002). Historical biogeography of the livebearing fish genus *Poeciliopsis* (Poeciliidae: Cyprinodontiformes). *Evolution*, *56*(5), 972–984. https://doi.org/10.1111/j.0014-3820.2002.tb01409.x

Matzke, N. J. (2013). Probabilistic historical biogeography: New models for founder-event speciation, imperfect detection, and fossils allow improved accuracy and model-testing. *Frontiers of Biogeography*, *5*(4), 242–248. https://doi.org/10.21425/f55419694

Matzke, N. J. (2014). Model selection in historical biogeography reveals that founder-event speciation is a crucial process in island clades. *Systematic Biology*, *63*(6), 951–970. https://doi.org/10.1093/sysbio/syu056

Mello, B., Tao, Q., Barba-Montoya, J., & Kumar, S. (2021). Molecular dating for phylogenies containing a mix of populations and species by using Bayesian and RelTime approaches. *Molecular Ecology Resources*, *21*(1), 122–136. https://doi.org/10.1111/1755-0998.13249

Mendoza, J., & Francke, O. (2017). Systematic revision of *Brachypelma* red-kneed tarantulas (Araneae: Theraphosidae), and the use of DNA barcodes to assist in the identification and conservation of CITES-listed species. *Invertebrate Systematics*, *31*(2), 157–179. https://doi.org/10.1071/IS16023

Mendoza, J., & Francke, O. (2020). Systematic revision of Mexican threatened tarantulas *Brachypelma* (Araneae: Theraphosidae: Theraphosinae), with a description of a new genus, and implications on the conservation. *Zoological Journal of the Linnean Society*, *188*(1), 82–147. https://doi.org/10.1093/zoolinnean/zlz046

Minh, B. Q., Schmidt, H. A., Chernomor, O., Schrempf, D., Woodhams, M. D., Von Haeseler, A., & Lanfear, R. (2020). IQ-TREE 2: New models and efficient methods for phylogenetic inference in the genomic era. *Molecular Biology and Evolution*, *37*(5), 1530–1534. https://doi.org/10.1093/molbev/msaa015

Morrone, J. J. (2020). *The Mexican Transition Zone: A natural biogeographic laboratory to study biotic assembly*. Springer. https://doi.org/10.1201/b21824-4

Morrone, J. J., Escalante, T., & Rodríguez-Tapia, G. (2017). Mexican biogeographic provinces: Map and shapefiles. *Zootaxa*, *4277*(2), 277–279. https://doi.org/10.11646/zootaxa.4277.2.8

Morrone, J. J., & Márquez, J. (2001). Halffter's Mexican Transition Zone, beetle generalized tracks, and geographical homology. *Journal of Biogeography*, *28*(5), 635–650. https://doi.org/10.1046/j.1365-2699.2001.00571.x

Muscarella, R., Galante, P. J., Soley-Guardia, M., Boria, R. A., Kass, J. M., Uriarte, M., & Anderson, R. P. (2014). ENMeval: An R package for conducting spatially independent evaluations and estimating optimal model complexity for Maxent ecological niche models. *Methods in Ecology and Evolution*, *5*(11), 1198–1205. https://doi.org/10.1111/2041-210x.12261

Nolasco-Soto, J., González-Astorga, J., Espinosa de los Monteros, A., Galante-Patiño, E., & Favila, M. E. (2017). Phylogeographic structure of *Canthon cyanellus* (Coleoptera: Scarabaeidae), a Neotropical dung beetle in the Mexican Transition Zone: Insights on its origin and the impacts of Pleistocene climatic fluctuations on population dynamics. *Molecular Phylogenetics and Evolution*, *109*, 180–190. https://doi.org/10.1016/j.ympev.2017.01.004

Olson, D. M., Dinerstein, E., Wikramanayake, E. D., Burgess, N. D., Powell, G. V. N., Underwood, E. C., D'Amico, J. A., Itoua, I., Strand, H. E., Morrison, J. C., Loucks, C. J., Allnutt, T. F., Ricketts, T. H., Kura, Y., Lamoreux, J. F., Wettengel, W. W., Hedao, P., & Kassem, K. R. (2001). Terrestrial ecoregions of the world: A new map of life on

Earth. *BioScience*, *51*(11), 933–938. https://doi.org/10.1641/0006-3568(2001)051[0933:teotwa]2.0.co;2

Otto-Bliesner, B. L., Marshall, S. J., Overpeck, J. T., Miller, G. H., Hu, A. & CAPE Last Interglacial Project members (2006). Simulating Arctic climate warmth and icefield retreat in the last interglaciation. *Science*, *311*(5768), 1751–1753. https://doi.org/10.1126/science.1120808

Paradis, E., Claude, J., & Strimmer, K. (2004). APE: Analyses of phylogenetics and evolution in R language. *Bioinformatics*, *20*(2), 289–290. https://doi.org/10.1093/bioinformatics/btg412

Phillips, S. J., Anderson, R. P., Dudík, M., Schapire, R. E., & Blair, M. E. (2017). Opening the black box: An open-source release of Maxent. *Ecography*, *40*(7), 887–893. https://doi.org/10.1109/IAW.2005.1496002

Phillips, S. J., Anderson, R. P., & Schapire, R. E. (2006). Maximum entropy modeling of species geographic distributions. *Ecological Modelling*, *190*(3–4), 231–259. https://doi.org/10.1016/j.ecolmodel.2005.03.026

Phillips, S. J., & Dudík, M. (2008). Modeling of species distributions with Maxent: New extensions and a comprehensive evaluation. *Ecography*, *31*(2), 161–175. https://doi.org/10.1111/j.2007.0906-7590.05203.x

Prendini, L., Weygoldt, P., & Wheeler, W. C. (2005). Systematics of the *Damon variegatus* group of African whip spiders (Chelicerata: Amblypygi): Evidence from behaviour, morphology and DNA. *Organisms, Diversity & Evolution*, *5*(3), 203–236. https://doi.org/10.1016/j.ode.2004.12.004

Pringle, E. G., Ramírez, S. R., Bonebrake, T. C., Gordon, D. M., & Dirzo, R. (2012). Diversification and phylogeographic structure in widespread *Azteca* plant-ants from the northern Neotropics. *Molecular Ecology*, *21*(14), 3576–3592. https://doi.org/10.1111/j.1365-294X.2012.05618.x

Qiao, H., Peterson, A. T., Campbell, L. P., Soberón, J., Ji, L., & Escobar, L. E. (2016). NicheA: Creating virtual species and ecological niches in multivariate environmental scenarios. *Ecography*, *39*(8), 805–813. https://doi.org/10.1111/ecog.01961

Quintero, D. (1980). Systematics and evolution of *Acanthophrynus* Kraepelin (Amblypygi, Phrynidae). In J. Grube (Ed.), *Verhandlungen. 8. Internationaler Arachnologen-Kongress abgehalten an der Universität für Bodenkultur Wien, 7–12 Juli, 1980* (pp. 341–347). H. Egermann.

R Core Team. (2012). *R: A language and environment for statistical computing*. R Foundation for Statistical Computing. http://www.r-project.org

Rengifo-Correa, L., Abad-Franch, F., Martínez-Hernández, F., Salazar-Schettino, P. M., Téllez-Rendón, J. L., Villalobos, G., & Morrone, J. J. (2021). A biogeographic–ecological approach to disentangle reticulate evolution in the *Triatoma phyllosoma* species group (Heteroptera: Triatominae), vectors of Chagas disease. *Journal of Zoological Systematics and Evolutionary Research*, *59*(1), 94–110. https://doi.org/10.1111/jzs.12409

Reveillion, F., Wattier, R., Montuire, S., Sousa Carvalho, L., & Bollache, L. (2020). Cryptic diversity within three South American whip spider species (Arachnida, Amblypygi). *Zoological Research*, *41*(5), 595–598. https://doi.org/10.24272/j.issn.2095-8137.2020.068

Ronquist, F., & Huelsenbeck, J. P. (2003). MrBayes 3: Bayesian phylogenetic inference under mixed models. *Bioinformatics*, *19*(12), 1572–1574. https://doi.org/10.1093/bioinformatics/btg180

Rull, V. (2008). Speciation timing and neotropical biodiversity: The Tertiary–Quaternary debate in the light of molecular phylogenetic evidence. *Molecular Ecology*, *17*(11), 2722–2729. https://doi.org/10.1111/j.1365-294X.2008.03789.x

Rull, V. (2011). Neotropical biodiversity: Timing and potential drivers. *Trends in Ecology and Evolution*, *26*(10), 508–513. https://doi.org/10.1016/j.tree.2011.05.011

Rundell, R. J., & Price, T. D. (2009). Adaptive radiation, nonadaptive radiation, ecological speciation and nonecological speciation. *Trends in Ecology & Evolution*, *24*(7), 394–399. http://dx.doi.org/10.1016/j.tree.2009.02.007

Schoener, T. W. (1968). The *Anolis* lizards of Bimini: Resource partitioning in a complex fauna. *Ecology*, *49*(4), 704–726. https://doi.org/10.2307/1935534

Schramm, F. D., Valdez-Mondragón, A., & Prendini, L. (2021). Volcanism and paleoclimate change drive diversification of world's largest whip spider (Amblypygi). *Dryad*. https://doi.org/10.5061/dryad.z612jm6b8

Seiter, M., Reyes Lerma, A. C., Král, J., Sember, A., Divišová, K., Palacios Vargas, J. G., Colmenares, P. A., Loria, S. F., & Prendini, L. (2020). Cryptic diversity in the whip spider genus *Paraphrynus* (Amblypygi: Phrynidae): Integrating morphology, karyotype and DNA. *Arthropod Systematics & Phylogeny*, *78*(2), 265–285. https://doi.org/10.26049/ASP78-2-2020-04

Sheldon, K. S., Huey, R. B., Kaspari, M., & Sanders, N. J. (2018). Fifty years of mountain passes: A perspective on Dan Janzen's classic article. *American Naturalist*, *191*(5), 553–565. https://doi.org/10.1086/697046

Shultz, J. W. (2007). A phylogenetic analysis of the arachnid orders based on morphological characters. *Zoological Journal of the Linnean Society*, *150*(2), 221–265. https://doi.org/10.1111/j.1096-3642.2007.00284.x

Simões, M., Breitkreuz, L., Alvarado, M., Baca, S., Cooper, J. C., Heins, L., Herzog, K., & Lieberman, B. S. (2016). The evolving theory of evolutionary radiations. *Trends in Ecology and Evolution*, *31*(1), 27–34. https://doi.org/10.1016/j.tree.2015.10.007

Smith, B. T., McCormack, J. E., Cuervo, A. M., Hickerson, M. J., Aleixo, A., Cadena, C. D., Pérez-Emán, J., Burney, C. W., Xie, X., Harvey, M. G., Faircloth, B. C., Glenn, T. C., Derryberry, E. P., Prejean, J., Fields, S., & Brumfield, R. T. (2014). The drivers of tropical speciation. *Nature*, *515*(7527), 406–409. https://doi.org/10.1038/nature13687

Sosa, V., De-Nova, J. A., & Vásquez-Cruz, M. (2018). Evolutionary history of the flora of Mexico: Dry forests cradles and museums of endemism. *Journal of Systematics and Evolution*, *56*(5), 523–536. https://doi.org/10.1111/jse.12416

Stevens, B., Giorgetta, M., Esch, M., Mauritsen, T., Crueger, T., Rast, S., Salzmann, M., Schmidt, H., Bader, J., Block, K., Brokopf, R., Fast, I., Kinne, S., Kornblueh, L., Lohmann, U., Pincus, R., Reichler, T., & Roeckner, E. (2013). Atmospheric component of the MPI-M Earth system model: ECHAM6. *Journal of Advances in Modeling Earth Systems*, *5*(2), 146–172. https://doi.org/10.1002/jame.20015

Stevens, G. C. (1989). The latitudinal gradient in geographical range: How so many species coexist in the tropics. *American Naturalist*, *133*(2), 240–256. https://doi.org/10.1086/284913

Stork, N. E. (2018). How many species of insects and other terrestrial arthropods are there on Earth? *Annual Review of Entomology*, *63*(1), 31–45. https://doi.org/10.1146/annurev-ento-020117-043348

Suárez-Atilano, M., Burbrink, F., & Vázquez-Domínguez, E. (2014). Phylogeographical structure within *Boa constrictor imperator* across the lowlands and mountains of Central America and Mexico. *Journal of Biogeography*, *41*(12), 2371–2384. https://doi.org/10.1111/jbi.12372

Van der Vaart, A. W. (1998). *Asymptotic statistics*. Cambridge University Press. https://doi.org/10.1017/CBO9780511802256

Vázquez, D. P., & Stevens, R. D. (2004). The latitudinal gradient in niche breadth: Concepts and evidence. *American Naturalist*, *164*(1), E1–E19. https://doi.org/10.1086/421445

Warren, D. L., Glor, R. E., & Turelli, M. (2008). Environmental niche equivalency versus conservatism: Quantitative approaches to niche evolution. *Evolution*, *62*(11), 2868–2883. https://doi.org/10.1111/j.1558-5646.2008.00482.x

Warren, D. L., Glor, R. E., & Turelli, M. (2010). ENMTools: A toolbox for comparative studies of environmental niche models. *Ecography*, *33*(3), 607–611. https://doi.org/10.1111/j.1600-0587.2009.06142.x

Weygoldt, P. (2000). *Whip spiders (Chelicerata: Amblypygi). Their biology, morphology and systematics*. Apollo Books.

Weyman, G. S. (1993). A review of the possible causative factors and significance of ballooning in spiders. *Ethology, Ecology and Evolution*, *5*(3), 279–291. https://doi.org/10.1080/08927014.1993.9523016

Wiens, J. J., & Donoghue, M. J. (2004). Historical biogeography, ecology and species richness. *Trends in Ecology and Evolution*, *19*(12), 639–644. https://doi.org/10.1016/j.tree.2004.09.011

Yu, Y., Blair, C., & He, X. (2020). RASP 4: Ancestral state reconstruction tool for multiple genes and characters. *Molecular Biology and Evolution*, *37*(2), 604–606. https://doi.org/10.1093/molbev/msz257

Yu, Y., Harris, A. J., Blair, C., & He, X. (2015). RASP (Reconstruct Ancestral State in Phylogenies): A tool for historical biogeography. *Molecular Phylogenetics and Evolution*, *87*, 46–49. https://doi.org/10.1016/j.ympev.2015.03.008

Zarza, E., Reynoso, V. H., & Emerson, B. C. (2008). Diversification in the northern Neotropics: Mitochondrial and nuclear DNA phylogeography of the iguana *Ctenosaura pectinata* and related species. *Molecular Ecology*, *17*(14), 3259–3275. https://doi.org/10.1111/j.1365-294X.2008.03826.x

Zarza, E., Reynoso, V. H., & Emerson, B. C. (2011). Discordant patterns of geographic variation between mitochondrial and microsatellite markers in the Mexican black iguana (*Ctenosaura pectinata*) in a contact zone. *Journal of Biogeography*, *38*(7), 1394–1405. https://doi.org/10.1111/j.1365-2699.2011.02485.x

Zarza, E., Reynoso, V. H., Faria, C. M. A., & Emerson, B. C. (2019). Introgressive hybridization in a spiny-tailed iguana, *Ctenosaura pectinata*, and its implications for taxonomy and conservation. *PeerJ*, *7*, e6744. https://doi.org/10.7717/peerj.6744

SUPPORTING INFORMATION

Additional supporting information may be found online in the Supporting Information section.

How to cite this article: Schramm FD, Valdez-Mondragón A, Prendini L. Volcanism and palaeoclimate change drive diversification of the world's largest whip spider (Amblypygi). *Mol Ecol*. 2021;30:2872–2890. https://doi.org/10.1111/mec.15924